SC.RR.69-297

9513

CID # 3824
CACC # 45-02

AEROSPACE NUCLEAR SAFETY

SC-RR-69-297
September 1969

TRAJECTORIES AND REENTRY ENVIRONMENTS FOR THE SNAP-27 GLFC DURING MULTIPLE REVOLUTION HIGHLY ELLIPTICAL ORBITAL DECAY AFTER SUPERCIRCULAR VELOCITY REENTRY

AEROSPACE RADIOISOTOPE POWER
INFORMATION CENTER
Accession No. 07410-02
Date DEC 17 1969
Sandia Laboratory

H. R. Spahr, 9513

AEROSPACE NUCLEAR SAFETY DEPARTMENT 9510

DO NOT DESTROY
Return to
AEROSPACE RADIOISOTOPE POWER
INFORMATION CENTER
Sandia Laboratory

SANDIA LABORATORIES

OPERATED FOR THE UNITED STATES ATOMIC ENERGY COMMISSION BY SANDIA CORPORATION | ALBUQUERQUE, NEW MEXICO. LIVERMORE, CALIFORNIA

Issued by Sandia Corporation,
a prime contractor to the
United States Atomic Energy Commission

LEGAL NOTICE

This report was prepared as an account of Government sponsored work. Neither the United States, nor the Commission, nor any person acting on behalf of the Commission:

A. Makes any warranty or representation, expressed or implied, with respect to the accuracy, completeness, or usefulness of the information contained in this report, or that the use of any information, apparatus, method, or process disclosed in this report may not infringe privately owned rights; or

B. Assumes any liabilities with respect to the use of, or for damages resulting from the use of any information, apparatus, method, or process disclosed in this report.

As used in the above, "person acting on behalf of the Commission" includes any employee or contractor of the Commission, or employee of such contractor, to the extent that such employee or contractor of the Commission, or employee of such contractor prepares, disseminates, or provides access to, any information pursuant to his employment or contract with the Commission, or his employment with such contractor.

SC-RR-69-297

TRAJECTORIES AND REENTRY ENVIRONMENTS FOR THE SNAP-27 GLFC DURING MULTIPLE REVOLUTION HIGHLY ELLIPTICAL ORBITAL DECAY AFTER SUPERCIRCULAR VELOCITY REENTRY

H. R. Spahr, 9513
Sandia Laboratories, Albuquerque

September 1969

DISTRIBUTED DEC 4, 1969

ABSTRACT

Trajectories and reentry environments are presented for the SNAP-27 Graphite Lunar Module Fuel Cask (GLFC) during multiple revolution highly elliptical orbital decay after shallow angle supercircular velocity reentry. The trajectories and reentry environments from a closed form approximate solution and from numerical integration of the equations of motion are compared for two of the eight perigee altitudes investigated.

The cutoff date for information in this report, with the exception of the 300,000 feet drag perigee TTA trajectory work, is October 29, 1968. The cutoff date for information in this report on the 300,000 feet drag perigee TTA trajectory work is May 19, 1969.

SUMMARY

In the Aerospace Nuclear Safety Program, safety analyses are required to determine the behavior of nuclear systems during launch aborts after liftoff and during reentries after use in space. These safety analyses are conducted for all nuclear systems designed for use in space.

As part of the Aerospace Nuclear Safety Program, the Sandia Laboratories Aerospace Nuclear Safety Department conducted a number of aerothermodynamic analyses of the SNAP-27 Graphite Lunar Module Fuel Cask (GLFC). These analyses included orbital decay reentries and prompt supercircular velocity reentries from translunar aborts.

After an Apollo mission abort during or after translunar injection, the SNAP-27 GLFC and lunar module (LM) can reenter the Earth's atmosphere at shallower than nominal reentry angles. For these very shallow reentry angles, the GLFC undergoes multiple revolution orbital decay from a highly elliptic orbit with apogee near the Moon.

This report summarizes the definitions of the trajectory and reentry environment for the SNAP-27 GLFC during such a multiple revolution highly elliptical orbital decay. The trajectory and reentry environment definition was part of an aerothermodynamic analysis performed to define the response of the SNAP-27 GLFC to such reentries.

TABLE OF CONTENTS

	Page
Introduction	9
GLFC and LM Configurations Analyzed	12
Computer Code HRS017	14
Trajectories and Reentry Environments From Computer Code HRS017	20
TTA Trajectory Code	22
Trajectories and Reentry Environments From the TTA Trajectory Code	26
Comparison of the Trajectories and Reentry Environments From the HRS017 and TTA Computer Codes	29
Definition of Minimum Reentry Angle for Prompt Supercircular Velocity Reentry	34
Conclusions	35
References	36
APPENDIX A -- LIST of QUIKTRAN Computer Code HRS017 (Version 1)	39
APPENDIX B -- Listing of FORTRAN Source Deck and Input Data for Computer Code HRS017 (Version 3)	45
APPENDIX C -- Trajectory and Reentry Environment Output From Computer Code HRS017 (Version 3) for a Perigee Altitude of 260,000 Feet (Five Revolutions)	57
1. Trajectory and Reentry Environment Tabulated Data	59
2. Listing of Punched Card CMA Input	64
APPENDIX D -- Trajectory and Reentry Environment Output From Computer Code HRS017 (Version 3) for a Perigee Altitude of 265,000 Feet (Ten Revolutions)	67
1. Trajectory and Reentry Environment Tabulated Data	69
2. Listing of Punched Card CMA Input	79
APPENDIX E -- Trajectory and Reentry Environment Output From Computer Code HRS017 (Version 3) for a Perigee Altitude of 270,000 Feet (Fourteen Revolutions)	83
1. Trajectory and Reentry Environment Tabulated Data	85
2. Listing of Punched Card CMA Input	99

TABLE OF CONTENTS
(continued)

	Page
APPENDIX F -- Trajectory and Reentry Environment Output From Computer Code HRS017 (Version 3) for a Perigee Altitude of 275,000 Feet (Eighteen Revolutions)	103
1. Trajectory and Reentry Environment Tabulated Data	105
2. Listing of Punched Card CMA Input	123
APPENDIX G -- Trajectory and Reentry Environment Output From Computer Code HRS017 (Version 3) for a Perigee Altitude of 285,000 Feet (Thirty Revolutions)	127
1. Trajectory and Reentry Environment Tabulated Data	129
2. Listing of Punched Card CMA Input	159
APPENDIX H -- Trajectory and Reentry Environment Output From Computer Code HRS017 (Version 3) for a Perigee Altitude of 290,000 Feet (Thirty-nine Revolutions)	163
1. Trajectory and Reentry Environment Tabulated Data	165
2. Listing of Punched Card CMA Input	204
APPENDIX I -- Trajectory and Reentry Environment Output From Computer Code HRS017 (Version 3) for a Perigee Altitude of 295,000 Feet (Fifty Revolutions)	209
1. Trajectory and Reentry Environment Tabulated Data	211
2. Listing of Punched Card CMA Input	261
APPENDIX J -- Trajectory and Reentry Environment Output From Computer Code HRS017 (Version 3) for a Perigee Altitude of 300,000 Feet (Sixty-Five Revolutions)	267
1. Trajectory and Reentry Environment Tabulated Data	269
2. Listing of Punched Card CMA Input	334
APPENDIX K -- Trajectory and Reentry Environment Output From the TTA Trajectory Computer Code for an Initial Drag Perigee of 259,570 Feet (Four Revolutions)	341
1. Listing of TTA Input Data	343
2. Trajectory and Reentry Environment Tabulated Data	345
3. Listing of Punched Card CMA Input	353

TABLE OF CONTENTS
(continued)

Page

APPENDIX L -- Trajectory and Reentry Environment Output From the TTA Trajectory Computer Code for an Initial Drag Perigee of 300,027 Feet (Twenty-Two Revolutions) 357

1. Listing of TTA Input Data 359

2. Trajectory and Reentry Environment Tabulated Data 363

3. Listing of Punched Card CMA Input 396

APPENDIX M -- Trajectory and Reentry Environment Output From the TTA Trajectory Computer Code for a -5.125 Degree Reentry Angle Prompt Reentry 401

1. Listing of TTA Input Data 403

2. Trajectory and Reentry Environment Tabulated Data 405

APPENDIX N -- Trajectory and Reentry Environment Output From the TTA Trajectory Computer Code for a -5.0625 Degree Reentry Angle Two Revolution Reentry 407

1. Listing of TTA Input Data 409

2. Trajectory and Reentry Environment Tabulated Data 411

TRAJECTORIES AND REENTRY ENVIRONMENTS FOR
THE SNAP-27 GLFC DURING MULTIPLE REVOLUTION
HIGHLY ELLIPTICAL ORBITAL DECAY AFTER
SUPERCIRCULAR VELOCITY REENTRY

Introduction

As part of the NASA Apollo program, the Apollo Lunar Surface Experiment Package (ALSEP) (Figure 1) will gather data regarding the characteristics and environment of the lunar surface and subsurface. References 1 and 2 describe, in some detail, the different experiments which are part of this package.

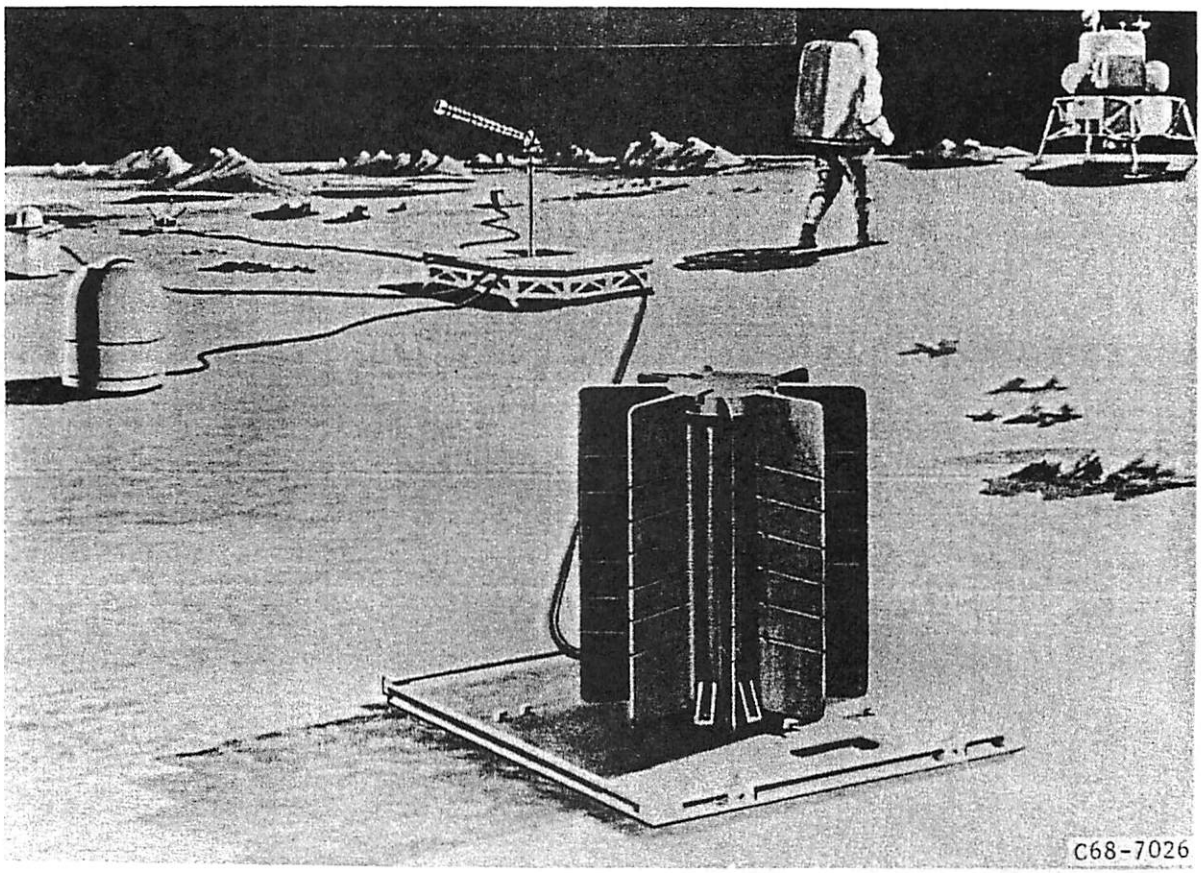

Figure 1. Apollo Lunar Surface Experiment Package array

The ALSEP package is designed to gather and transmit data for a 1-year period. The AEC developed the SNAP-27 radioisotope thermoelectric generator (RTG) to supply electrical power for the ALSEP package. The General Electric Co. (GE) designed and fabricated the SNAP-27 generator, fuel capsule, and Graphite Lunar Module Fuel Cask (GLFC) under AEC contract.

The SNAP-27 fuel capsule (Figure 2) is contained in the GLFC (Figure 3) during transport to the lunar surface. Titanium struts and bands attach the GLFC to the lunar module.

As part of the Aerospace Nuclear Safety Program, the Reentry and Space Sciences Division of Sandia Laboratories had conducted a number of aerodynamic and thermodynamic analyses of the original SNAP-27 beryllium fuel cask and fuel capsule.[3,4] In Reference 4, it was shown that the SNAP-27 beryllium fuel cask and fuel capsule, as originally designed:

1. would not survive all supercircular velocity lunar return reentries, even if separated from the lunar module (LM) at high altitudes, and
2. could survive orbital decay reentries from circular Earth orbits if separated from the LM at high altitudes.

The information presented in Reference 4 was contained in a presentation made by the Aerospace Nuclear Safety Department of Sandia Laboratories at the Atomic Energy Commission Headquarters on November 4, 1966.

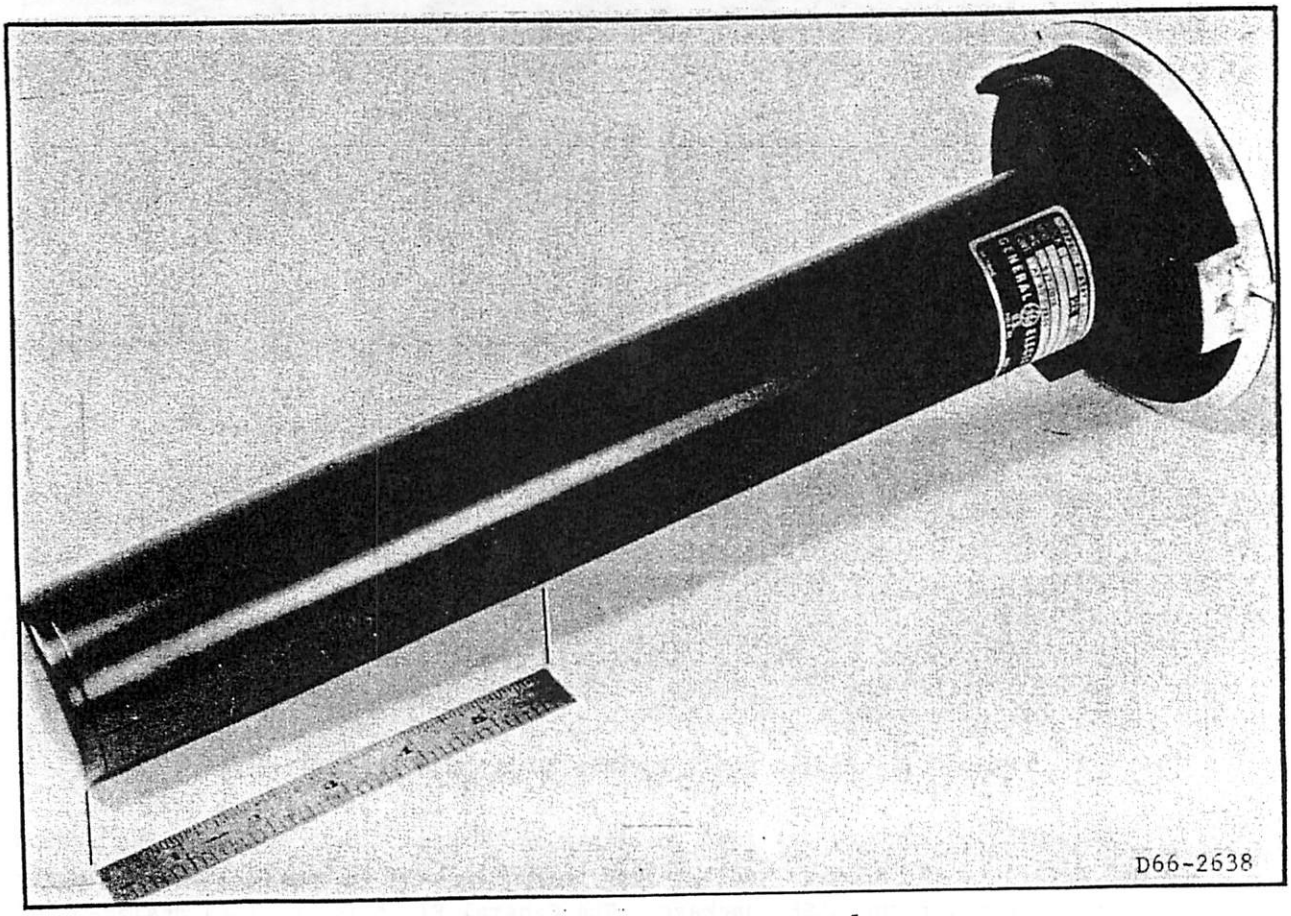

Figure 2. SNAP-27 fuel capsule

As is done for all SNAP systems for space use, the Reentry and Space Sciences Division of the Sandia Laboratories Aerospace Nuclear Safety Department conducted a number of aerothermodynamic analyses of the SNAP-27 GLFC and attached hardware during the GE design of the GLFC. (Two of these analyses are documented in References 8 and 9.) These analyses included orbital decay reentries and prompt supercircular velocity reentries from translunar aborts. However, after an Apollo mission abort during or after translunar injection, the SNAP-27 GLFC and LM can reenter the Earth's atmosphere at shallower than nominal reentry angles. For these very shallow reentry angles, the GLFC and LM undergo multiple revolution orbital decay from a highly elliptical orbit with apogee near the Moon.

In meetings of the Reentry Working Group of the SNAP-27/ALSEP Interagency Safety Review Panel, questions were raised by panel members regarding:

1. The temperature response of the SNAP-27 GLFC to the multiple revolution orbital decay described above.
2. The ablation of the SNAP-27 GLFC during the multiple revolution orbital decay described above.
3. The reentry angle which separates prompt reentries from the multiple revolution orbital decay described above.

Mr. Elliott Katzen, Chairman of the Reentry Working Group, requested that the Sandia Reentry and Space Sciences Division perform an aerothermodynamic analysis to answer these questions. This analysis was started on September 23, 1968, and was completed by October 28, 1968. The results were presented at the Reentry Working Group meeting at Valley Forge, Pennsylvania, October 29 through 31, 1968.

This report documents the orbital mechanics and trajectory analyses of the aerothermodynamic analysis which defined:

1. The trajectories and reentry environments for the SNAP-27 GLFC and LM during the multiple revolution orbital decay described previously.
2. The reentry angle which separates prompt reentries from the multiple revolution orbital decay described previously.

GLFC and LM Configurations Analyzed

The pertinent LM configuration from translunar aborts, as defined by NASA Manned Spacecraft Center personnel, is the ascent and descent stages together, all fuel tanks 100 percent full. For this analysis, this configuration was assumed to reenter crosswise. For this orientation, the official NASA Manned Spacecraft Center data[10] are:

Weight = 32,963.6 pounds
C_D = 3.2 (constant)
Reference area = 129.4 square feet

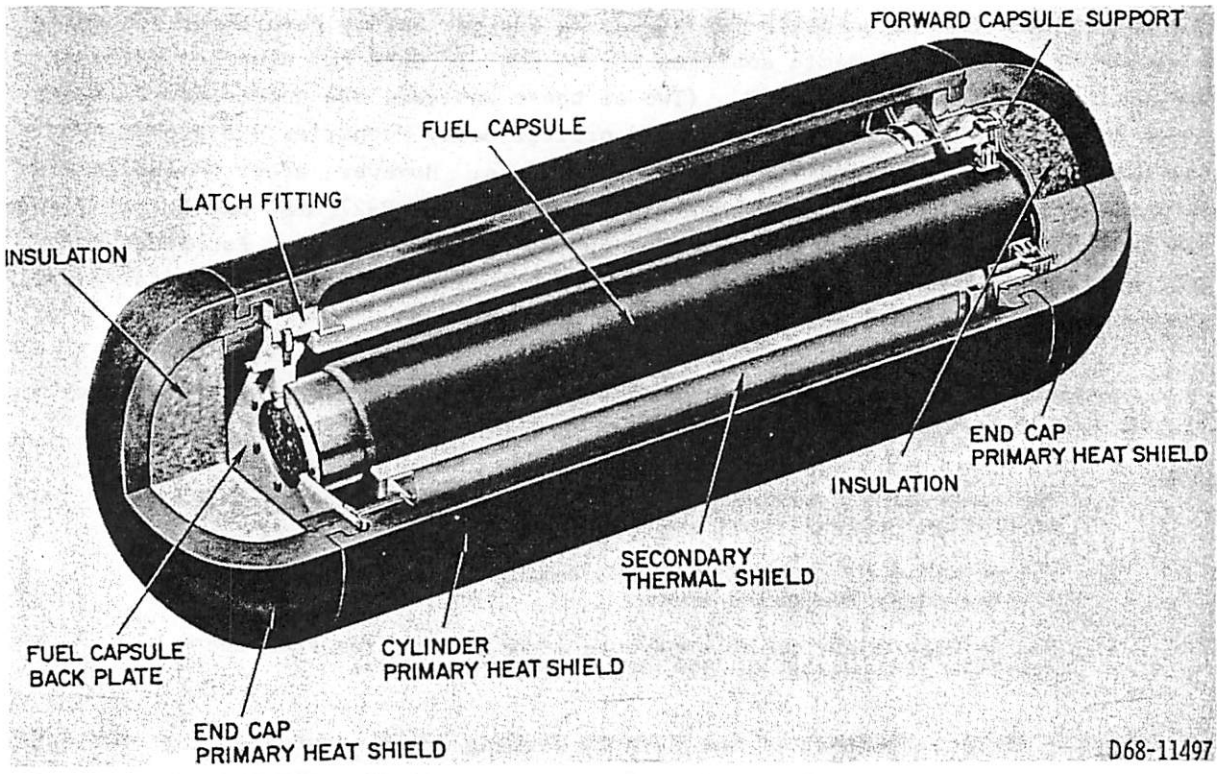

Figure 3. SNAP-27 Graphite Lunar Module Fuel Cask (GLFC) (cutaway view)

Based on probability information obtained by the Safety Analysis Division of Sandia Laboratories, the probability of supercircular velocity reentries is the same order of magnitude as the probability of orbital decay reentries. Thus, it was necessary to design a fuel cask which would also survive the supercircular velocity reentries.

A previous Reentry and Space Sciences Division analysis[5] had shown the feasibility of using a graphite heat shield to contain a fuel capsule during the orbital decay reentry environment. (Reference 6 presents more recent work on the same subject.) At the request of the AEC Space Electric Power Office (SEPO), the Sandia Reentry and Space Sciences Division started a study of the feasibility of using a graphite fuel cask to contain the SNAP-27 fuel capsule. The analysis was started December 15, 1966; the results were contained in a presentation made by Sandia Laboratories Aerospace Nuclear Safety Department personnel at AEC Headquarters on January 5, 1967. (Reference 7 documents the aerodynamic and trajectory analyses conducted for this study.)

Based on the results of this analysis and a somewhat similar analysis by GE, AEC/SEPO directed GE to redesign the fuel cask to survive both orbital decay and supercircular velocity reentries. Thus, GE designed the GLFC.

This corresponds to a constant ballistic coefficient of 79.607 pounds per square foot. (Reference 10, which superseded Reference 11, does not present separate drag coefficients for the free molecule and continuum flow regimes.) The above data are for Lunar Module 5, without the landing legs.

The GLFC external configuration is a right circular cylinder with axisymmetric elliptical end caps which are almost hemispherical.[12] Total overall length is 23 inches, and the cylindrical diameter is 8 inches. The GLFC weight, with the fuel capsule installed, is 40 pounds.

The variation of hypersonic drag coefficient (based on a reference area of 0.3491 square foot) with altitude for the GLFC reentering crosswise is presented below from previous Reentry and Space Sciences Division calculations. At the request of Mr. Elliott Katzen, the GLFC was assumed to reenter crosswise stable with no oscillatory motion. Thus, the GLFC reentry response calculated represents the upper bounds on the ablation and maximum external temperature response of the GLFC for the actual oscillatory motion during the multiple revolution reentry. These drag coefficient data also are presented in Figure 4, where the Sandia Laboratories drag coefficient data are compared with GE drag coefficient data for the GLFC.

Geometric Altitude Above Mean Sea Level (ft)	Hypersonic Drag Coefficient (C_D)
400,000.0	7.39
325,000.0	7.39
300,000.0	5.70
270,000.0	4.23
0.0	4.23

The GLFC aerothermodynamic analyses required the trajectory and reentry environment only during the severe or high velocity part of the reentry, so the aerodynamic model for the GLFC did not include supersonic, transonic, or subsonic aerodynamic data.

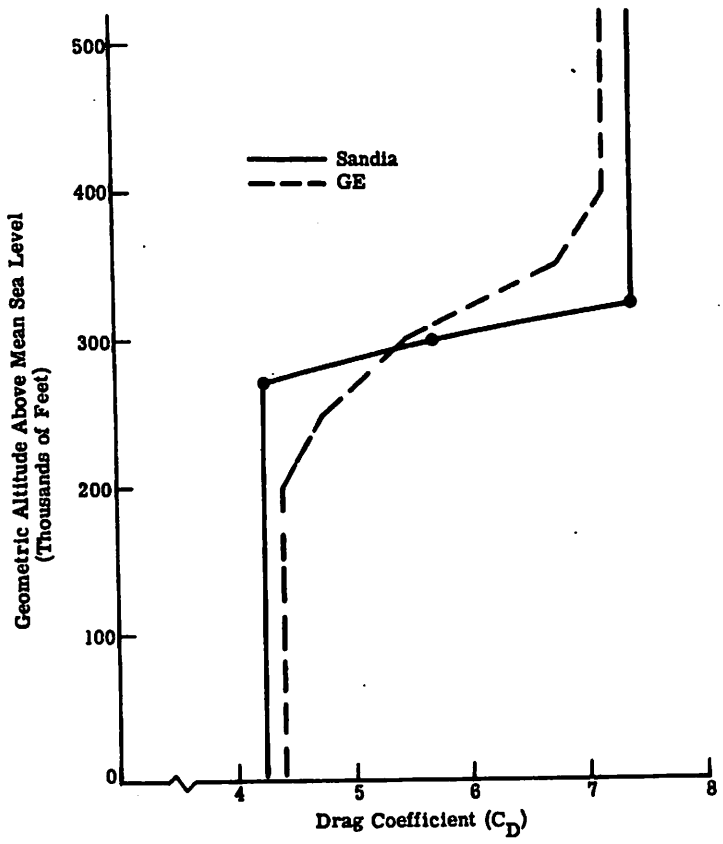

Figure 4. GLFC hypersonic flow drag coefficient as a function of altitude, crosswise reentry

Computer Code HRS017

The highly elliptical Earth orbits examined in this analysis have orbital periods measured in days. As is shown later, the perigee altitude range of interest corresponds to many revolutions during the orbital decay process. Thus, the orbital decay process occurs during a time period measured in days or months.

Ideally, a complex trajectory code including the Earth, lunar, and solar gravitational fields would be used to numerically integrate the differential equations of motion for the orbital decay process; or, as an approximation, a trajectory code such as the Sandia Laboratories TTA trajectory code[13-15] which contains only the Earth's gravitational field could be used to numerically integrate the differential equations of motion for the orbital decay process. Unfortunately, either of the above methods would require computer times measured in hours. Computer time of such duration is available only on weekends, and the analysis would have been limited to one run per week. Also, use of existing computer codes would result in an output format which would require either intermediate manual calculation and

key punching or an additional computer code to provide punched card input data in the required format for use with the Charring Materials Ablation (CMA) code.[16] The CMA code was used in the aerothermodynamic analysis to define surface recession as a function of time for the GLFC.

To eliminate the above restrictions on the analysis, which would result if numerical integration of the differential equations of motion were done, computer code HRS017 was written. Computer code HRS017 uses a closed form approximate solution for the orbital decay of an object initially in an elliptical orbit. The closed form approximate solution uses a Keplerian elliptical orbit to define the trajectory for each revolution. Perigee altitude is assumed to be constant during the orbital decay. At the apogee of each revolution, a step change in apogee radius is made, with the change in apogee radius, Δr_a, defined by:

$$\Delta r_a = -\sqrt{2\pi}\,\frac{C_D A}{W}\,\frac{\rho_p}{\sqrt{\beta}}\,\frac{r_a\left(r_a + r_p\right)}{\sqrt{\dfrac{r_a - r_p}{2}}} \tag{1}$$

where

Δr_a = change in apogee radius per revolution, feet

π = 3.14157, dimensionless

C_D = hypersonic drag coefficient of the object at perigee altitude, dimensionless

A = aerodynamic reference area of the object, square feet

W = weight of the object, pounds

ρ_p = atmospheric density at perigee altitude, pounds per cubic foot

β = atmospheric density exponential for an exponential atmosphere, evaluated at perigee, per foot

r_a = distance from the object to the center of the Earth when the object is at apogee, apogee radius, feet

r_p = distance from the object to the center of the Earth when the object is at perigee, perigee radius, feet

References 17 and 18 discuss in detail the development of Eq. (1). The required assumptions in the development were:

1. The change in orbital size and shape per orbit is very small.
2. The eccentricity of the initial undisturbed orbit is assumed equal to or greater than 0.05.
3. The perigee radius remains constant while the apogee radius decreases.
4. The Earth has a spherically symmetric gravitational field which is defined by an inverse square field.
5. The Earth is spherical in shape.

6. The Earth's atmosphere is spherically symmetric and is an exponential atmosphere.

7. The effects of the rotation of the Earth's atmosphere with the Earth are neglected, i.e., the air relative velocity is assumed equal to the inertial velocity of the object.

8. The object has a constant ballistic parameter, W/C_DA, during the region of interest near perigee.

9. The eccentricity of the orbit, squared, is much less than one.

10. The inertial velocity of the object in its elliptical orbit is assumed constant at the inertial velocity at perigee.

11. The incremental distance at any point in the orbit can be approximated by the perigee radius times the incremental central range angle.

12. The difference between apogee altitude and perigee altitude must remain larger than approximately 5 times the atmospheric scale height.

13. The gravitational fields of the Moon and Sun were ignored.

Some of the assumptions in the development are, of necessity, violated. For the class of highly elliptical orbits being examined, assumption 9 is violated except for the final few orbits. Assumption 12 is violated for the final few orbits for the higher perigee altitudes because these orbits become almost circular. Also, assumption 3 is violated because the perigee radius decreases during the decay process.

The results of the closed form approximate solution computer code are compared in a later section with the results of the TTA code. This comparison defines the validity of using the closed form approximate solution. One would expect the approximate solution, because of the assumption of constant perigee height, to:

1. Predict a larger number of orbits than does the "exact" solution.

2. Have lower heating rates in the later orbits than does the "exact" solution.

These two effects tend to compensate in ablation analyses.

The closed form approximate solution computer code calculates pertinent parameters at selected values of the central range angle, θ, around the orbit. The equations required[19-22] to define the radius from the center of the Earth, the altitude above the spherical Earth, the velocity, and the geocentric reentry angle are:

$$r = \frac{2r_a r_p}{\left(r_a + r_p\right) + \left(r_a - r_p\right) \cos \theta} \tag{2}$$

where

r = distance from the object to the center of the Earth, feet

θ = central range angle of the object from perigee, degrees

and

$$h = r - r_e \tag{3}$$

where

h = geocentric geometric altitude of the object above the spherical Earth, feet

r_e = radius of the spherical Earth, feet

and

$$V = \sqrt{\mu\left(\frac{2}{r} - \frac{1}{a}\right)} \tag{4}$$

where

V = inertial and air relative velocity of the object, feet per second

μ = Earth spherical gravitational field constant, feet^3 per second^2

a = semimajor axis of the orbit = $(r_a + r_p)/2$, feet

and

$$\gamma = \text{arc cos}\sqrt{\frac{r_a r_p}{r\left(r_a + r_p - r\right)}} \tag{5}$$

where

γ = geocentric reentry angle, radians.

The pertinent equations used to calculate the time at each point around the orbit are:

$$e = \frac{r_a - r_p}{r_a + r_p} \tag{6}$$

where

e = orbital eccentricity, dimensionless

and

$$E = \text{arc cos}\left(\frac{e + \cos\theta}{1 + e\cos\theta}\right) \tag{7}$$

where

E = eccentric anomaly, radians

and

$$\Delta t = \sqrt{\frac{a^3}{\mu}}(E - e \sin E) \tag{8}$$

where

Δt = time increment from perigee, seconds.

The pertinent equations for aerodynamic heating are:

$$QFM = \frac{C_1 \rho V^3}{50,063} \tag{9}$$

where

QFM = free molecule flow stagnation point heating rate to the object, Btu per square foot second

C_1 = thermal accommodation coefficient, dimensionless

ρ = atmospheric density at the altitude h, pounds per cubic foot

and

$$QCONT = 865\ C_2\left(\frac{\rho}{\rho_{SL}}\right)^{0.5}\left(\frac{V}{10,000}\right)^{3.15} \quad \text{(Reference 23)} \tag{10}$$

where

QCONT = continuum flow stagnation point heating rate to the object, Btu per square foot second

C_2 = constant which includes the effects of the square root of the object nose radius on the heating as well as the effect of the shape of the object on the heating, dimensionless

ρ_{SL} = sea level atmospheric density, pounds per cubic foot.

The stagnation pressure at the stagnation point on the object is calculated by:

$$P_T = \frac{\rho V^2}{32.2} \tag{11}$$

where

P_T = stagnation pressure at the stagnation point of the object, pounds per square foot.

The preceding 11 equations define the trajectory and reentry environment parameters for the object decaying from orbit. Version 1 of computer code HRS017 solves these equations. This version was written in QUIKTRAN[24] and made operational on the Sandia Laboratories QUIKTRAN remote terminal. The remote terminal is linked by phone lines to an IBM 7040/44 computer in Los Angeles. Use of the

remote terminal with "instant access" to a computer provided the quickest way to write the code, make the code operational, and provide preliminary results for the analysis. Appendix A contains a QUIKTRAN "LIST" of version 1 of computer code HRS017. The output from version 1 of computer code HRS017 is similar to the printed output of version 3.

The equations below define the additional reentry environment input data required by the CMA code:

$$P_{T_A} = \frac{P_T}{2116.4} \tag{12}$$

where

P_{T_A} = stagnation pressure at the stagnation point of the object, atmospheres

and

$$H_R = \frac{V^2}{50,063} \tag{13}$$

where

H_R = stagnation enthalpy at the stagnation point of the object, Btu per pound

Version 2 of the code was written in FORTRAN[25] for use on the Sandia CDC 3600. This code basically consisted of version 1, with the slight changes required in converting from QUIKTRAN to FORTRAN. The stagnation point convective heating rate, QDOTC, was defined as the free molecule value, QFM, above a specified altitude and as the continuum value, QCONT, below the specified altitude. The correct PUNCH format statement was added to punch the required CMA computer code input into a card deck in a format compatible with the CMA computer code. Cards were punched for all the points around the orbit.

Version 3 of the computer code is identical to version 2, with three changes. The stagnation point heating rate, QDOTC, is more realistically defined as the minimum value of QFM and QCONT. The time punched in the data deck is the time for each orbit from the first point around the orbit where the altitude is below 1,000,000 feet. Version 3 punches CMA computer code input cards only for those points in the orbit where the altitude is below 1,000,000 feet.

Appendix B contains a listing of the FORTRAN source deck of version 3 of computer code HRS017. The source deck listed is used on a CDC 6600 computer. Other source decks of this code are operational on a CDC 3600 and a Univac 1108. Output from version 3 of computer code HRS017 is contained in Appendices C through J and is discussed later.

Computer code HRS017 is not discussed in detail in this report. This computer code will be documented in a separate report.

Trajectories and Reentry Environments From Computer Code HRS017

Version 1 of computer code HRS017, operational on the Sandia QUIKTRAN remote terminal, was used for preliminary calculations to define the perigee altitude range of interest. The results of two preliminary runs are summarized below.

Preliminary Run 1 - lunar module free molecule W/C_DA, perigee altitude of 245,000 feet, decayed after 10 revolutions

Preliminary Run 2 - lunar module free molecule W/C_DA, perigee altitude of 240,000 feet, decayed after 6 revolutions

The free molecule ballistic coefficient data in Reference 7 were used for the lunar module descent stage, side forward orientation. After revising the ballistic coefficient to reflect current lunar module weights, the ballistic coefficient was 79.607. The official NASA lunar module aerodynamic data[10,11] were not available at the time of these calculations. In the actual reentry, the ballistic coefficient of the lunar module changes from the lower ballistic coefficient of free molecule flow at the higher altitudes to the higher ballistic coefficient of continuum flow at the lower altitudes. The approximate closed form theory, however, permits use of only one value of the ballistic coefficient for the computations.

These two preliminary computations show that the lunar module would make multiple revolution reentries at perigee altitudes as low as 240,000 feet. However, based on the NASA predicted lunar module disassembly altitude of 300,000 feet, the lunar module would disassemble prior to perigee for perigee altitudes of less than 300,000 feet. Thus, the pertinent configuration for almost all of each of the multiple revolution reentries is the GLFC alone.

Since the GLFC alone is the pertinent configuration for almost all of each of the multiple revolution reentries, the following two preliminary computations were made.

Preliminary Run 3 - GLFC continuum W/C_DA = 27.008 pounds per square foot, perigee altitude of 260,000 feet, decayed after five orbits

Preliminary Run 4 - GLFC continuum W/C_DA = 27.008 pounds per square foot, perigee altitude of 255,000 feet, decayed after one orbit

The continuum W/C_DA of the GLFC was used because the perigee altitude was low enough that the GLFC was in continuum flow at perigee.

These four preliminary runs showed that:

1. The perigee altitude range of interest is from 260,000 feet to 300,000 feet. (Perigee altitudes above 300,000 feet are not of interest because the GLFC would still be on the lunar module and experience reduced heating in continuum flow due to the larger lunar module dimensions.)

2. The pertinent configuration for this perigee altitude range for most of the multiple revolution reentry is the GLFC alone.

Thus, computer code HRS017, version 3, was used to compute the trajectory and reentry environment for the GLFC alone for the following perigee altitudes:

1. Perigee altitude = 260,000 feet, GLFC W/C_DA = 27.008 pounds per square foot, decayed in 5 revolutions.

2. Perigee altitude = 265,000 feet, GLFC W/C_DA = 27.008 pounds per square foot, decayed in 10 revolutions.

3. Perigee altitude = 270,000 feet, GLFC W/C_DA = 27.008 pounds per square foot, decayed in 14 revolutions.

4. Perigee altitude = 275,000 feet, GLFC W/C_DA = 25.576 pounds per square foot, decayed in 18 revolutions.

5. Perigee altitude = 285,000 feet, GLFC W/C_DA = 23.054 pounds per square foot, decayed in 30 revolutions.

6. Perigee altitude = 290,000 feet, GLFC W/C_DA = 21.992 pounds per square foot, decayed in 39 revolutions.

7. Perigee altitude = 295,000 feet, GLFC W/C_DA = 21.005 pounds per square foot, decayed in 50 revolutions.

8. Perigee altitude = 300,000 feet, GLFC W/C_DA = 20.102 pounds per square foot, decayed in 65 revolutions.

(The GLFC W/C_DA's above were evaluated at the perigee altitude.) The results of these computations are presented in Appendices C through J.

Part 1 of Appendices C through J contains tabulations of the trajectory and reentry environments which are printed out. The parameters printed out are:

TIME	-	time from the start of the multiple revolution reentry, seconds
THETA	-	central range angle from perigee, degrees
ALTITUDE	-	geometric altitude above the spherical Earth model, feet
GAMMA	-	magnitude of the geocentric inertial reentry angle, degrees
QCONT	-	continuum aerodynamic stagnation point cold wall heating rate, Btu per square foot second
QFM	-	free molecule aerodynamic stagnation point cold wall heating rate, Btu per square foot second
V	-	inertial and air relative velocity, feet per second
P_T	-	stagnation pressure at the stagnation point, pounds per square foot

Part 2 of Appendices C through J contains listings of the punched card reentry environment outputs which are used as inputs for the CMA ablation code. (To minimize the number of pages in this report, the listings contain only those revolutions used in the CMA computer code and the ablation analysis.) Cards have been inserted in the decks to provide revolution identification and column headings. The parameters listed are:

TIME	-	time from the first point computed in the orbit which is below 1,000,000 feet altitude, seconds
H_R	-	stagnation point total enthalpy, Btu per pound
QDOTR	-	radiative aerodynamic stagnation point heating rate, Btu per square foot second
$QDOTC/H_R$	-	convective aerodynamic stagnation point cold wall heating rate, QDOTC, divided by the stagnation point total enthalpy, H_R, pounds per square foot second
P_{T_A}	-	stagnation pressure at the stagnation point, atmospheres
I.D.	-	object identification

(Computer code HRS017 sets QDOTR to 0 because the radiative heating to the SNAP-27 GLFC is negligible for the altitude and velocity ranges which exist in the multiple orbit problem.)

The convective aerodynamic stagnation point cold wall heating rate histories for the decaying GLFC are summarized in Figures 5 through 8. These figures present the convective aerodynamic stagnation point cold wall heating rate as a function of time from perigee for the first and next to last revolutions for four different perigee altitudes. Figures 5 through 8 correspond to perigee altitudes of 260,000 feet (5 revolutions), 270,000 feet (14 revolutions), 285,000 feet (30 revolutions), and 300,000 feet (65 revolutions).

TTA Trajectory Code

The TTA trajectory program (Theoretical Trajectory program A) was developed in 1961 to provide a versatile tool to generate theoretical trajectories in support of Sandia Laboratories activities. Since late 1961, this code has been used to compute over 20,000 reentry, rocket-boosted, and free-fall trajectories in support of various weapons programs, research activities, and the Aerospace Nuclear Safety Program. The TTA program is continually being revised and updated to increase its capabilities and flexibility.

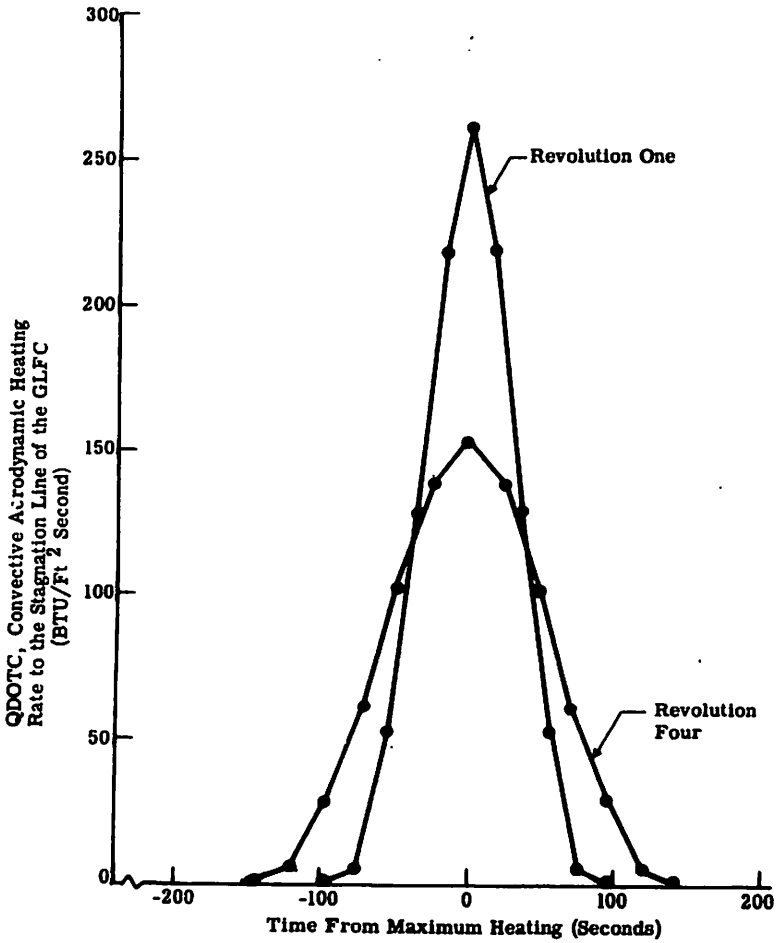

Figure 5. Convective aerodynamic heating rate to the stagnation line of the GLFC as a function of time for the first and fourth revolutions, perigee altitude = 260,000 feet (five revolutions), HRS017 computer code

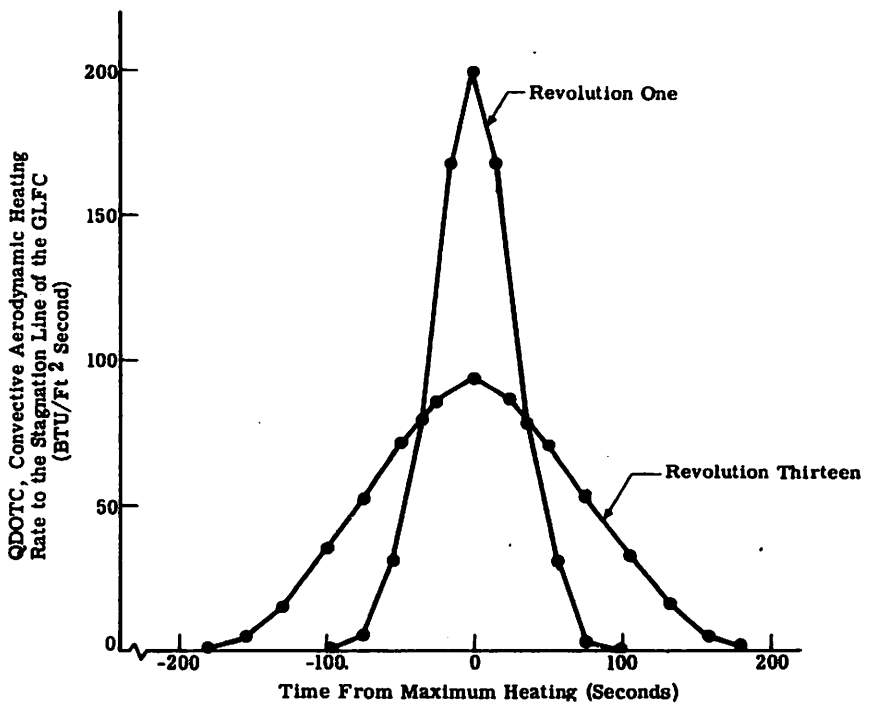

Figure 6. Convective aerodynamic heating rate to the stagnation line of the GLFC as a function of time for the first and thirteenth revolutions, perigee altitude = 270,000 feet (fourteen revolutions), HRS017 computer code

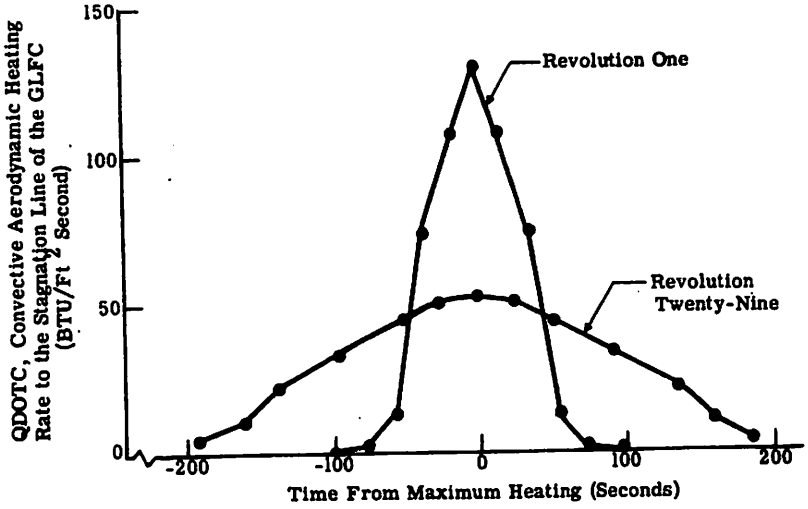

Figure 7. Convective aerodynamic heating rate to the stagnation line of the GLFC as a function of time for the first and twenty-ninth revolutions, perigee altitude = 285,000 feet (thirty revolutions), HRS017 computer code

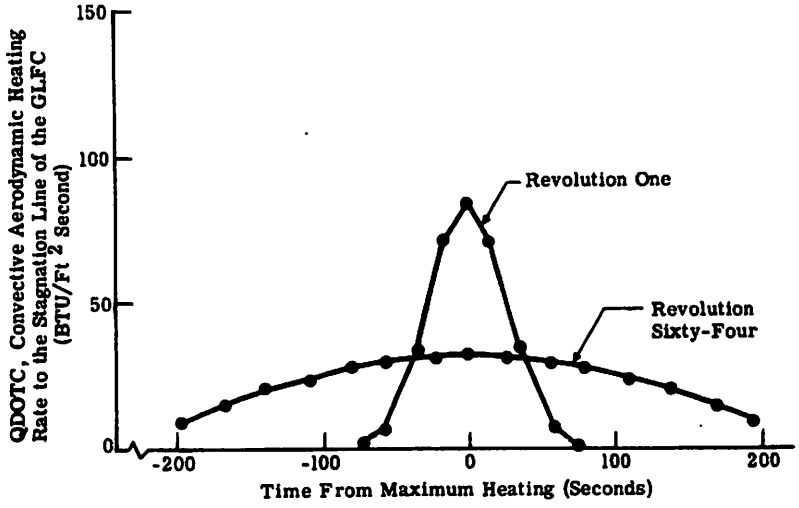

Figure 8. Convective aerodynamic heating rate to the stagnation line of the GLFC as a function of time for the first and sixty-fourth revolutions, perigee altitude = 300,000 feet (sixty-five revolutions), HRS017 computer code

The TTA program numerically integrates the equations of motion for a rigid object flying a 6-degree-of-freedom trajectory in the vicinity of the Earth. (However, only the point mass 3-degree-of-freedom option was used for the trajectories presented in this report.) The integration subroutine uses a modified Adams-Moulton predictor corrector method of order two (parabolic). The numerical integration time step size is controlled by an automatic mesh control system.

The rigid object may be subjected to all the aerodynamic forces and moments (including magnus forces and moments) and to the thrust, Earth gravitational field, buoyancy forces, and arbitrary external forces and moments acting on the object while moving relative to a rotating oblate Earth. The object's weight, aerodynamic coefficients, thrust, and arbitrary external forces and moments may be defined as variable functions of from one to three computed parameters.

The atmospheric models currently used have properties that are functions of height alone and rotate with the Earth. Provisions are available for including wind velocities in the atmospheric models.

The only gravitational field in the TTA computer code is that of the oblate rotating Earth. This gravitational field includes the second gravitational harmonic.

The Earth is described as an oblate spheroid with a polar radius of 20,855,107 feet and an equatorial radius of 20,925,540 feet. The rotational rate of the Earth is $7.29211513186 \times 10^{-5}$ radians per second.

The input data to the code can be either inertial or Earth relative. Coordinates, while normally in a geodetic system, can be expressed either in a geocentric system or in a Cartesian coordinate system. Output data can be either inertial or Earth relative. Approximately 250 parameters are available as output data. The TTA code is currently being used on a CDC 3600 electronic computer.

The results of the Sandia Laboratories TTA program have been successfully compared with the results of trajectory codes used by the Air Force Special Weapons Center, AVCO Corporation, Atomics International, General Electric, Ling Temco Vought Corporation, Lockheed, and the National Aeronautics and Space Administration. References 13, 14, and 15 provide detailed descriptions of the Sandia Laboratories TTA code.

Trajectories and Reentry Environments From the TTA Trajectory Code

The Sandia Laboratories TTA computer code was used to compute the trajectory and reentry environments for the SNAP-27 GLFC for multiple revolution orbital decay from two initial perigee altitudes to check the accuracy of the closed form approximate solution used in computer code HRS017. The results of these computations are presented in Appendices K and L, as discussed below.

The initial conditions for the first TTA trajectory were:

Inertial velocity = 35,910.7 feet per second

Inertial geodetic reentry angle = -6.9730 degrees

Inertial heading angle (counterclockwise from east is positive) = -90.0 degrees

Geometric geodetic altitude above mean sea level = 578,068.0 feet

Geodetic latitude = 14.0 degrees

Longitude = 0.0 degree

These initial conditions were transformed to the TTA coordinate system from a point calculated by the HRS017-3 computer code. This point was on the first revolution, prior to entering the atmosphere, of the 260,000 feet perigee altitude calculation.

The first trajectory had an initial drag perigee altitude of 259,570 feet. The lunar module aerodynamic data presented previously were used until an altitude of 273,000 feet was first reached. (The altitude of 273,000 feet was used because the latest lunar module disassembly altitude information[10] had not arrived when this TTA trajectory was computed. The difference in lunar module disassembly altitude between the 273,000 feet used here and the later value of 300,000 feet used in the other TTA trajectory would be small because the lunar module disassembles prior to or at perigee on the first revolution.) Then the GLFC aerodynamic data presented previously were used to impact. (The portion of the trajectory presented in Appendix K where the Mach number is below 3 should be ignored, since only hypersonic aerodynamic data were used for the GLFC.)

Part 1 of Appendix K contains a listing of the TTA trajectory code input for the first trajectory. Part 2 of Appendix K contains the tabulated trajectory and reentry environment computed for the first trajectory. Part 3 of Appendix K contains a listing of the punched card CMA input.

The trajectory and reentry environment parameters presented are:

HITE - geometric geodetic altitude above mean sea level, feet

LAT - geodetic latitude, degrees

LONG - longitude, degrees

Q	-	dynamic pressure, pounds per square foot
VT	-	air relative velocity, feet per second
MACH	-	Mach number, dimensionless
GAMMA	-	air relative geodetic reentry angle, degrees
TAU	-	angle between the Earth relative velocity vector and east, positive counterclockwise, degrees
AT	-	acceleration along the flight path, g
DQC	-	continuum flow aerodynamic convective heating reference rate at the stagnation point of a 1-foot radius sphere, Btu per square foot second
QC	-	time integral of DQC, Btu per square foot
RADVC	-	distance from the center of the Earth, feet
RHO	-	atmospheric density, pounds per cubic foot
TIME	-	time from the start of the reentry, seconds
CD	-	drag coefficient, dimensionless

Figure 9 presents the convective aerodynamic heating rate to the stagnation line of the GLFC as a function of time for the first and third revolutions from the first trajectory.

Preliminary computer runs for the second trajectory (initial perigee altitude ≈300,000 feet) indicated that large amounts of computer time (10 to 15 hours) would be required to compute the trajectory, and that detectable errors from computer roundoff and finite step size would exist if the entire trajectory were to be computed. Thus, the logic in the TTA computer code was used only to compute the portion of the trajectory in the Earth's atmosphere.

The initial conditions for the second TTA trajectory were:

Inertial velocity = 35,947.7 feet per second

Inertial geodetic reentry angle = -5.9785 degrees

Inertial heading angle (counterclockwise from east is positive) = -90.0 degrees

Geometric geodetic altitude above mean sea level = 533,724.7 feet

Geodetic latitude = 12.07881 degrees

Longitude = 0.0 degree

These initial conditions were transformed to the TTA coordinate system from a point calculated by the HRS017-3 computer code. This point was on the first revolution, prior to entering the atmosphere, of the 300,000 feet perigee altitude calculation.

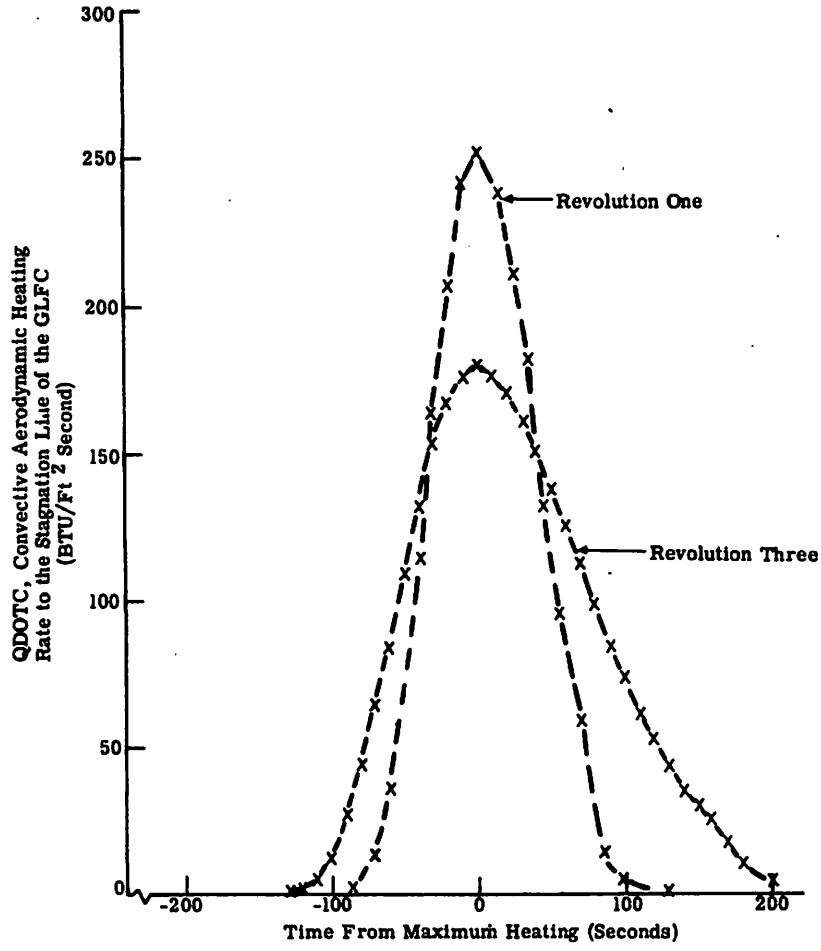

Figure 9. Convective aerodynamic heating rate to the stagnation line of the GLFC as a function of time for the first and third revolutions, initial perigee altitude ≈ 260,000 feet (four revolutions), TTA computer code

The second trajectory had an initial drag perigee altitude of 300,027 feet. The lunar module aerodynamic data presented previously were used until an altitude of approximately 300,000 feet was first reached. Then the GLFC aerodynamic data presented previously were used to impact. (The portion of the trajectory presented in Appendix L where the Mach number is below 3 should be ignored, since only hypersonic aerodynamic data were used for the GLFC.)

Part 1 of Appendix L contains a listing of the TTA trajectory code input for the second trajectory. Part 2 of Appendix L contains the tabulated trajectory and reentry environment computed for the first trajectory. Part 3 of Appendix L contains a listing of the punched card CMA input.

Figure 10 presents the convective aerodynamic heating rate to the stagnation line of the GLFC as a function of time for the first and twenty-first revolutions of the second trajectory.

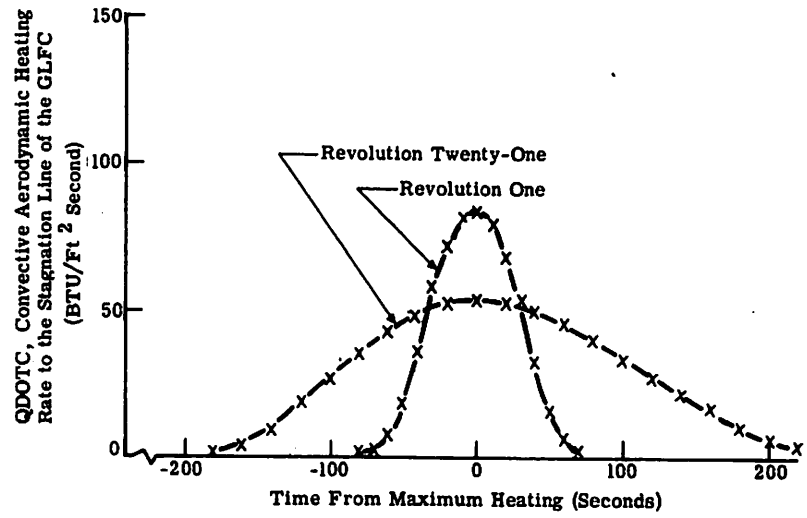

Figure 10. Convective aerodynamic heating rate to the stagnation line of the GLFC as a function of time for the first and twenty-first revolutions, initial perigee altitude ≈ 300,000 feet (twenty-two revolutions), TTA computer code

Comparison of the Trajectories and Reentry Environments From the HRS017 and TTA Computer Codes

The first comparison of the results of the HRS017 and TTA computer codes was for the minimum initial perigee altitude of approximately 260,000 feet. For this case, the HRS017 code showed that the GLFC reentered on the fifth revolution while the TTA code showed that the GLFC reentered on the fourth revolution.

Figure 11 presents the convective aerodynamic heating rate to the stagnation line of the GLFC as a function of time for the first revolution computed by the HRS017 and TTA computer codes for an initial perigee altitude of approximately 260,000 feet. Examination of Figure 11 shows that the two codes computed almost identical heating rate histories for the first revolution.

Figure 12 presents the convective aerodynamic heating rate to the stagnation line of the GLFC as a function of time for the fourth revolution computed by the HRS017 computer code and for the third revolution computed by the TTA computer code for an initial perigee altitude of approximately 260,000 feet. (These revolutions are the next-to-the-last revolution for each method of computation. The last revolutions, during which the GLFC reenters, are not compared because the orbital decay equations obviously break down on the last revolution.) Examination of Figure 12 shows that the two codes computed heating rate histories which are similar for the

next-to-the-last revolutions. The TTA computer code, which predicted reentry on the fourth revolution, has a higher heating rate history on the next-to-the-last revolution than does the HRS017 computer code, which predicted reentry on the fifth revolution.

The results shown in Figures 11 and 12 were expected because the HRS017 computer code uses a constant perigee and the TTA computer code computes the actual decaying perigee The drag perigee altitudes for successive revolutions from the TTA computer code results were:

Revolution 1 - drag perigee altitude ≈ 259,570 feet

Revolution 2 - drag perigee altitude ≈ 255,980 feet

Revolution 3 - drag perigee altitude ≈ 250,750 feet

Revolution 4 - reentered on fourth revolution

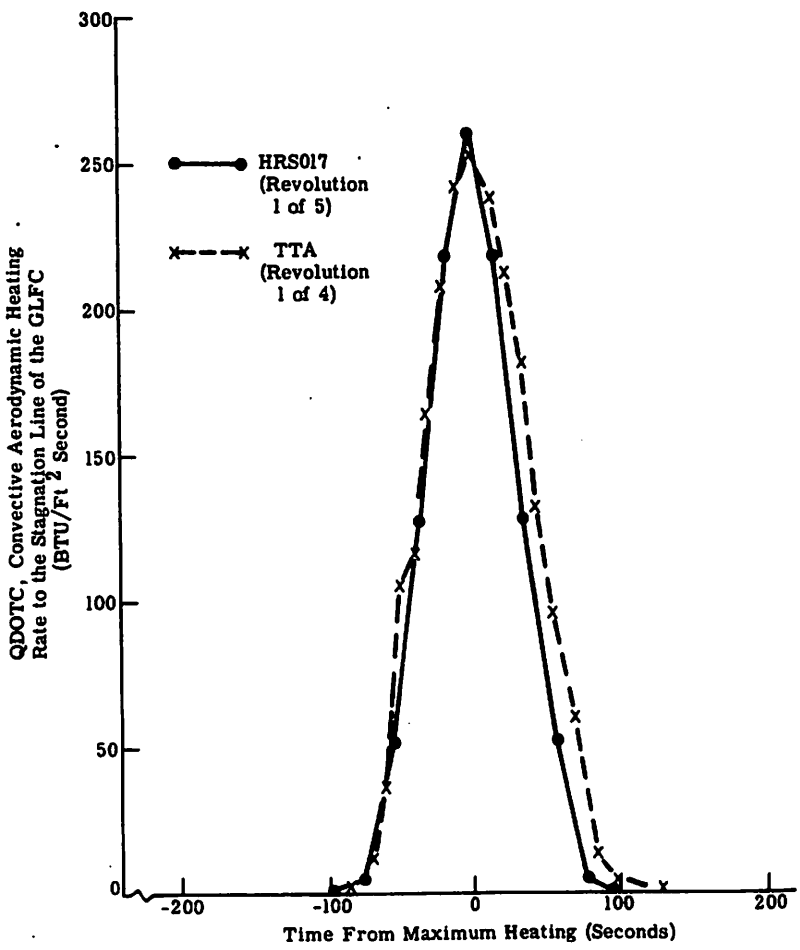

Figure 11. Convective aerodynamic heating rate to the stagnation line of the GLFC as a function of time for the first revolution from the HRS017 and TTA computer codes, initial perigee altitude ≈ 260,000 feet

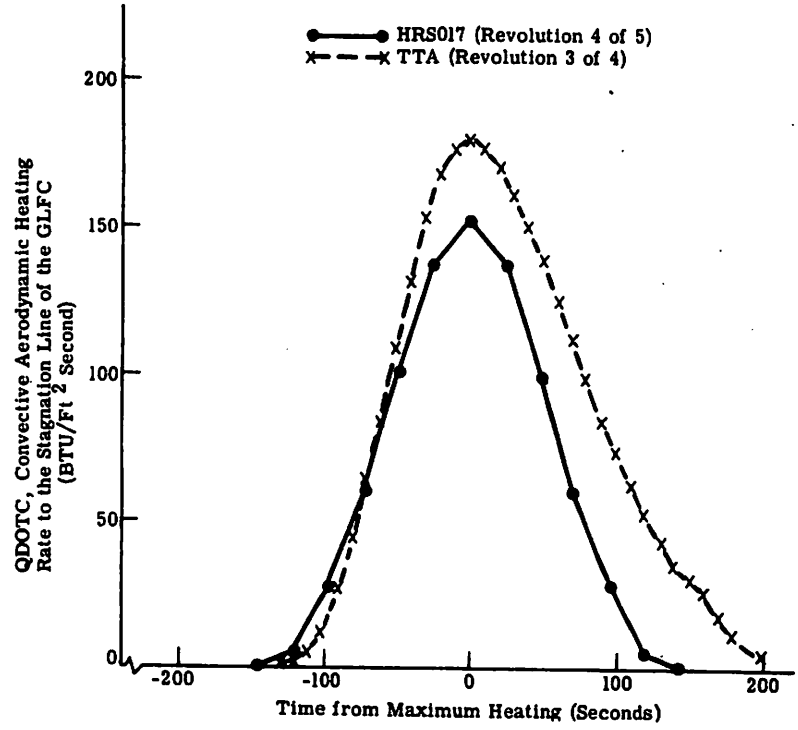

Figure 12. Convective aerodynamic heating rate to the stagnation line of the GLFC as a function of time for the next-to-the-last revolution from the HRS017 and TTA computer codes, initial perigee altitude ≈ 260,000 feet

Figures 11 and 12 show that the aerodynamic heating rate histories calculated for the GLFC by computer codes HRS017 and TTA are quite similar. Examination of the tabular data in Appendices C and K shows that the histories of other pertinent ablation parameters are quite similar for the two methods of computation.

Ablation calculations, documented in Reference 27, were made for the GLFC using the reentry environments computed by the HRS017 and TTA computer codes for an initial perigee altitude of 260,000 feet. (Reentry environments from a previously computed GLFC and LM orbital decay trajectory were used with the HRS017 reentry environment.) The resultant total ablations at the stagnation point of the GLFC (crosswise stable, no roll) were:

HRS017 reentry environment input (4 revolutions + orbital decay) = 0.180 inch ablation

HRS017 reentry environment input (5 revolutions + orbital decay) = 0.210 inch ablation

TTA reentry environment input = 0.189 inch ablation

Some questions exist as to whether the HRS017 results for the final revolution should be included in the ablation analyses. Therefore, the ablation calculations using the HRS017 reentry environment input were computed with and without the final revolution.

Figure 13 presents the convective aerodynamic heating rate to the stagnation line of the GLFC as a function of time for the first revolution computed by the HRS017 and TTA computer codes for an initial perigee altitude of approximately 300,000 feet. Examination of Figure 13 shows that the two codes computed almost identical heating rate histories for the first revolution.

Figure 14 presents the convective aerodynamic heating rate to the stagnation line of the GLFC as a function of time for the sixty-fourth revolution computed by the HRS017 computer code and for the twenty-first revolution computed by the TTA computer code for an initial perigee altitude of approximately 300,000 feet. (These revolutions are the next-to-the-last revolution for each method of computation. The last revolutions, during which the GLFC reenters, are not compared because the orbital decay equations obviously break down on the last revolution.)

Examination of Figure 14 shows that the two codes computed heating rate histories which are similar for the next-to-the-last revolution. The TTA computer code, which predicted reentry on the twenty-second revolution, has a higher heating rate history on the next-to-the-last revolution than does the HRS017 computer code, which predicted reentry on the sixty-fifth revolution.

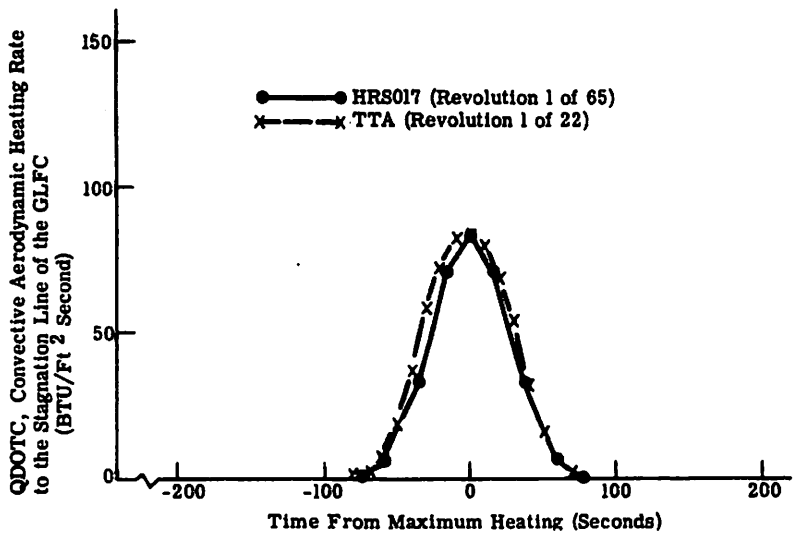

Figure 13. Convective aerodynamic heating rate to the stagnation line of the GLFC as a function of time for the first revolution from the HRS017 and TTA computer codes, initial perigee altitude ≈ 300,000 feet

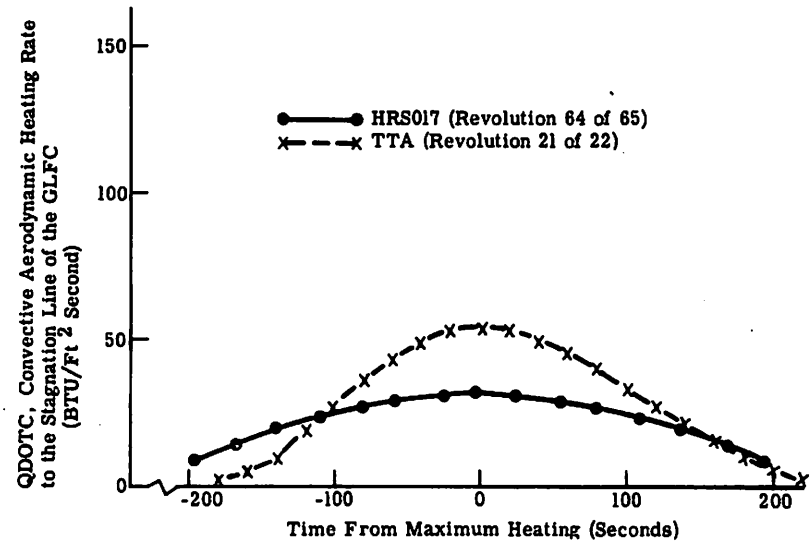

Figure 14. Convective aerodynamic heating rate to the stagnation line of the GLFC as a function of time for the next-to-the-last revolution from the HRS017 and TTA computer codes, initial perigee altitude ≈ 300,000 feet

The results shown in Figures 13 and 14 were expected because the HRS017 computer code uses a constant perigee and the TTA computer code computes the actual decaying perigee. The drag perigee altitudes for several revolutions from the TTA computer code results were:

Revolution 1 - drag perigee altitude ≈ 300,027 feet

Revolution 6 - drag perigee altitude ≈ 298,832 feet

Revolution 11 - drag perigee altitude ≈ 297,162 feet

Revolution 16 - drag perigee altitude ≈ 294,273 feet

Revolution 21 - drag perigee altitude ≈ 284,222 feet

Revolution 22 - reentered on twenty-second revolution

Figures 13 and 14 show that the aerodynamic heating rate histories calculated for the GLFC by computer codes HRS017 and TTA are similar. Examination of the tabular data in Appendices J and L shows that the histories of other pertinent ablation parameters are similar for the two methods of computation.

Ablation calculations, documented in Reference 27, were made for the GLFC using the reentry environments computed by the HRS017 and TTA computer codes for an initial perigee altitude of 300,000 feet. The same techniques described previously were used in the HRS017 reentry environment ablation calculations. The resultant total ablations at the stagnation point of the GLFC (crosswise stable, no roll) were:

HRS017 reentry environment input (64 revolutions + orbital decay) = 0.472 inch ablation

HRS017 reentry environment input (65 revolutions + orbital decay) = 0.483 inch ablation

TTA reentry environment input = 0.285 inch ablation

Examination of the ablation calculation results for a perigee altitude of 260,000 feet shows that the HRS017 reentry environment results in a calculated ablation approximately 20 percent higher than the TTA reentry environment results. For a perigee altitude of 300,000 feet, examination of the ablation calculation results shows that the HRS017 reentry environment results in a calculated ablation approximately 40 percent higher than the TTA reentry environment results.

Definition of Minimum Reentry Angle for Prompt Supercircular Velocity Reentry

The TTA trajectory code was used to compute five supercircular velocity reentry trajectories to define the reentry angle boundary between prompt and multiple revolution reentries. These five trajectories had inertial geodetic reentry angles of -5.0, -5.5, -5.25, -5.125, and -5.0625 degrees.

The initial conditions, other than reentry angles, were the same for all the trajectories and were:

Inertial velocity = 36,050.0 feet per second

Inertial heading angle (counterclockwise from east is positive) = -90.0 degrees

Geometric geodetic altitude above mean sea level = 400,000.0 feet

Geodetic latitude = 0.0 degree

Longitude = 0.0 degree

The lunar module aerodynamic model, discussed previously, was used down to an altitude of 273,000 feet. (These trajectories were computed before the NASA/MSC lunar module disassembly information in Reference 10 was received.) The GLFC aerodynamic model was then used down to impact.

The trajectory with a reentry angle of -5.125 degrees reentered promptly, while the trajectory with a reentry angle of -5.0625 degrees reentered on the second revolution. Thus, the bounding reentry angle between prompt reentry and multiple revolution reentry was defined as -5.09 ± 0.03 degrees.

Appendices M and N present the results for the trajectories with reentry angles of -5.125 and -5.0625 degrees; these angles are just on each side of the bounding reentry angle between prompt reentry and multiple revolution reentry.

Part 1 of Appendices M and N presents a listing of the TTA trajectory input data. Part 2 of each appendix presents the tabulated trajectory and reentry environment data. The tabulated reentry parameters were defined in a previous section of this report. (The portions of the trajectories presented in Appendices M and N where the Mach number is below 3 should be ignored, as only hypersonic aerodynamic data were used for the GLFC.)

Conclusions

This report has presented and discussed the reentry environments for the SNAP-27 GLFC during multiple revolution orbital decay after shallow angle supercircular velocity reentry. The reentry environments were defined for eight initial perigee altitudes using the HRS017 and TTA computer codes. The reentry angle boundary between prompt reentry and multiple-revolution reentry was also defined.

Based on the analyses and results documented in this report, and the ablation analysis in Reference 27, the following conclusions are drawn.

1. The pertinent initial perigee range of interest for the GLFC multiple revolution reentry problem is the altitude range from 260,000 to 300,000 feet.

2. Since the lunar module disassembles the first time it reaches 300,000 feet, the GLFC is the pertinent configuration for almost all of the multiple revolution reentry.

3. The HRS017 and TTA computer codes compute similar reentry environments for the same initial conditions. As would be expected, the HRS017 computer code calculates more revolutions during the reentry and lower heating rate histories for the later orbits than does the TTA computer code.

4. For the specified orientation (side-on stable, no roll), multiple revolution reentry is the most severe reentry mode for ablation.

5. Ablation calculations, using the reentry environments from computer codes HRS017 and TTA, show that the HRS017 reentry environment predicts 20 to 40 percent more ablation than does the TTA reentry environment.

6. The bounding inertial geodetic reentry angle at 400,000 feet between prompt and multiple revolution reentry of the GLFC is -5.09 ± 0.03 degrees.

These results and conclusions with the exception of the 300,000 feet initial perigee altitude TTA trajectory and corresponding ablation calculations, were presented at the Reentry Working Group meeting at Valley Forge, Pennsylvania, October 29 through 31, 1968.

References

1. W. J. Normyle, "NASA Given Lunar Surface Experiment Demonstration," Aviation Week and Space Technology, July 25, 1966.

2. R. D. Hibben, "ALSEP Array Cut for First Moon Missions," Aviation Week and Space Technology, April 3, 1967.

3. SC-RR-66-611, Aerothermodynamic Analysis of the SNAP-27 Fuel Cask, S. McAlees, Jr., R. D. Klett, B. E. Pearce, D. W. Larson, J. T. Stephens, and H. R. Spahr, Sandia Laboratories, Albuquerque, New Mexico, September 1966, (SDO).

4. SC-RR-66-2651, Aerothermodynamic and Structural Analysis of the SNAP-27 Fuel Cask, R. E. Berry, R. D. Klett, D. W. Larson, and H. R. Spahr, Sandia Laboratories, Albuquerque, New Mexico, January 1967 (OUO) (SDO).

5. Internal Sandia Laboratories Memo, R. D. Klett, 9314, to S. McAlees, Jr., 9314, Feasibility of SNAP-19 Intact Reentry (U), July 7, 1966 (CRD) (copies to AEC/SEPO).

6. SC-RR-67-197, Thermal Design of a SNAP-19 Generator for Intact Reentry, R. D. Klett, Sandia Laboratories, Albuquerque, New Mexico, April 1967.

7. SC-RR-67-150, Aerodynamic and Trajectory Analyses of a SNAP-27 Graphite Fuel Cask, H. R. Spahr, Sandia Laboratories, Albuquerque, New Mexico, May 1967 (OUO) (SDO).

8. SC-RR-67-2961, An Analysis of the Increased Aerodynamic Heating to the SNAP-27 Graphite Lunar Module Fuel Cask (GLFC) Resulting From the Titanium Mounting Structure, H. R. Spahr, Sandia Laboratories, Albuquerque, New Mexico, February 1968.

9. SC-RR-68-208, Thermal Analysis of a SNAP-27 Graphite Fuel Cask, D. W. Larson, Sandia Laboratories, Albuquerque, New Mexico, July 1968 (OUO).

10. NASA MSC Memorandum, R. S. Morton to Aerodynamics and Flight Dynamics Subsystems Manager, Re: Extreme Altitude Aerodynamic Drag Coefficients for the LM and the LM-S IV B, September 19, 1968, ET 253/6809-147-B (enclosure to letter from C. C. Kraft, Jr., NASA MSC, to S. McAlees, Jr., 9314, Sandia Laboratories, Re: Transmittal of Lunar Module Aerodynamic Drag Coefficient Data, October 2, 1968, 68-FM37-411).

11. TRW Note No. 68-FMT-673, Preliminary Report for SNAP-27 Environmental and Safety Analysis (Project Technical Report Task A-188.1), TRW Systems, Houston, Texas, July 29, 1968.

12. G. E. Isotopes Space Power Organization, Drawing 47 E 3011 34, Code Identification No. 15227, Sheet 2, Revision F, dated July 3, 1968, GLFC Assembly.

13. SC-DR-65-511, The TTA Generalized Rigid Body Trajectory Program for Digital Computer, J. A. F. Allensworth, Sandia Laboratories, Albuquerque, New Mexico, August 1966.

14. SC-DR-65-271, An Introduction to the TTA Generalized Rigid Body Trajectory Program for Digital Computer, J. A. F. Allensworth, Sandia Laboratories, Albuquerque, New Mexico, May 1965.

15. SC-RR-66-22, A Comparison of the Results of the Sandia Corporation TTA Trajectory Program and the Atomics International RESTORE Trajectory Program, H. R. Spahr, Sandia Laboratories, Albuquerque, New Mexico, February 1966.

16. SC-M-66-377, Operating Instructions for Charring Material Ablation Code, F. W. Bolek and D. F. McVey, Sandia Laboratories, Albuquerque, New Mexico, August 1966.

17. Sandia Laboratories Internal Memo, H. R. Spahr, 9312, to A. J. Clark, Jr., 9312, Re: Closed Form Approximate Solution for the Ballistic Parameter Required for Controlled De-Orbiting of Nuclear Systems from Elliptical Orbits Using Deployable Drag Devices, January 11, 1966.

18. Course Notes, Flight Mechanics of Spacecraft, University of Michigan, Ann Arbor, Michigan, July 1965.

19. A. E. Roy, The Foundations of Astrodynamics, The Macmillan Co., New York, 1965.

20. R. M. L. Baker, Jr., and M. W. Makemson, An Introduction to Astrodynamics, Academic Press, New York, 1967.

21. R. M. L. Baker, Jr., Astrodynamics: Applications and Advanced Topics, Academic Press, New York, 1967.

22. J. Jensen, G. Townsend, J. Kork, and D. Kraft, Design Guide to Orbital Flight, McGraw-Hill Book Co., Inc., New York, 1962.

23. R. W. Detra and H. Hidalgo, "Generalized Heat Transfer Formulas and Graphs for Nose Cone Re-Entry Into the Atmosphere," American Rocket Society Journal, March 1961.

24. IBM, Data Processing Application E 20-0240-0, Information Marketing QUIKTRAN User's Guide, International Business Machines Corporation, White Plains, New York, 1965.

25. 3400 - 3600 Computer Systems FORTRAN Reference Manual, Control Data Corporation, Palo Alto, California, September 1965.

26. U. S. Standard Atmosphere, 1962, U. S. Government Printing Office, Washington D.C., December 1962.

27. SC-RR-69-353, Ablation and Thermal Response of the SNAP-27 GLFC During Multiple Orbit Reentry, D. W. Larson, Sandia Laboratories, Albuquerque, New Mexico, to be published.

APPENDIX A

LIST of QUIKTRAN Computer
Code HRS017 (Version 1)

```
QUIKTRAN AT YOUR SERVICE
LN05  READY ;USER[redacted]
101. -READY       LOAD(HRS017)
235. +READY       LIST
101. =       CF    PROGRAM HRS017
102. =       C     (WRITTEN BY HAROLD R. SPAHR, DIVISION 9513, SANDIA CORPORATION,
103. =       C     SANDIA BASE, ALBUQUERQUE, NEW MEXICO - PHONE 264-1040, BUILDING
104. =       C     892, ROOM 233, HOME PHONE 299-5465)
105. =       C     THIS IS VERSION ONE OF HRS017. THIS VERSION IS OPERATIONAL ON THE
106. =       C     SANDIA CORPORATION QUIKTRAN REMOTE TERMINAL LINKED BY PHONE LINES
107. =       C     TO AN IBM 7040/44 COMPUTER IN LOS ANGELES.
108. =             DIMENSION ALT(500),RHO(500),AID(11),AIDD(11)
109. =             XK1=6.2832**0.5
110. =             III=0
111. =             XMU=1.4098E16
112. =             IRSUBE=20925697
113. =             RSUBE=IRSUBE
114. =             GO TO 188
115. =         189 READ 8,(AID(I),I=1,11)
116. =             READ 7,I1
117. =           7 FORMAT(7X,I3)
118. =             READ 4,(ALT(J),RHO(J),J=1,I1)
119. =           4 FORMAT(F9.0,7X,E10.3)
120. =         188 READ 8,(AIDD(I),I=1,11)
121. =           8 FORMAT(11A6)
122. =             READ 100,WCDA
123. =             READ 100,XHITEP
124. =             READ 106,RSUBA
125. =         106 FORMAT(E12.3)
126. =         100 FORMAT(F15.1)
127. =             TIME=0.0
128. =             L=1
129. =         110 IF(XHITEP-ALT(L))123,122,121
130. =         122 RHX=RHO(L)
131. =             M=L-1
132. =             ALTD=ALT(M)-ALT(L)
133. =             RATIO=RHO(M)/RHO(L)
134. =             ALOGR=ALOG(RATIO)
135. =             XBETA=ALOGR/(-ALTD)
136. =             GO TO 124
137. =         121 M=L-1
138. =             IF(XHITEP-ALT(M))181,182,183
139. =         183 L=L-1
140. =             GO TO 121
141. =         182 RHX=RHO(M)
142. =             ALTD=ALT(M)-ALT(L)
143. =             RATIO=RHO(M)/RHO(L)
144. =             ALOGR=ALOG(RATIO)
145. =             XBETA=ALOGR/(-ALTD)
146. =             GO TO 124
147. =         181 ALTD=ALT(M)-ALT(L)
148. =             RATIO=RHO(M)/RHO(L)
149. =             ALOGR=ALOG(RATIO)
150. =             XBETA=ALOGR/(-ALTD)
151. =             POWER=-(XBETA*ALT(L))
152. =             RHOSS=RHO(L)/EXP(POWER)
153. =             POWER2=-(XBETA*XHITEP)
154. =             RHX=RHOSS*EXP(POWER2)
```

```
      GO TO 124
  123 L=L+1
      GO TO 110
  124 CONTINUE
      RHY=RHX
  175 CONTINUE
      THETA=-180.0
      JJ=0
  150 CONTINUE
      RSUBP=RSUBE+XHITEP
      B=RSUBA+RSUBP
      C=RSUBA-RSUBP
      D=THETA/57.29578
      E=COS(D)
      F=2.0*RSUBA/(B+C*E)
      R=RSUBP*F
      XHITE=R-RSUBE
   77 IF(XHITE)188,15,15
   15 CONTINUE
   60 IF(XHITE-ALT(L))73,72,71
   72 RHX=RHO(L)
      GO TO 74
   71 M=L-1
      IF(M-1)161,161,162
  161 RHX=0.0
      GO TO 74
  162 IF(XHITE-ALT(M))171,172,173
  173 L=L-1
      GO TO 71
  172 RHX=RHO(M)
      GO TO 74
  171 ALTD=ALT(M)-ALT(L)
      RATIO=RHO(M)/RHO(L)
      ALOGR=ALOG(RATIO)
      BETA=ALOGR/(-ALTD)
      POWER=-(BETA*ALT(L))
      RHOSS=RHO(L)/EXP(POWER)
      POWER2=-(BETA*XHITE)
      RHX=RHOSS*EXP(POWER2)
      GO TO 74
   73 L=L+1
      GO TO 60
   74 CONTINUE
      X=RSUBP/(RSUBA+RSUBP-R)
      Y=RSUBA/R
      Z=(X*Y)**0.5
      GAMMA=ARCOS(Z)
      GAMMAD=GAMMA*57.29578
      AAA=B/2.0
      XN=1.0/(AAA**3.0/XMU)**0.5
      V=(XMU*(2.0/R-1.0/AAA))**0.5
      QCONT=865.0*(RHX/0.076474)**0.5*(V/10000.0)**3.15
      QFM=RHX*V**3.0/50063.0
      EE=C/B
      EEE=ARCOS(0.999999*((AAA-R)/(AAA*EE)))
      T2=(EEE-EE*SIN(EEE))/XN
      DT=ABS(T2-T1)
      IF(JJ)133,133,134
  133 DT=0.0
```

```
214. =        134 CONTINUE
215. =            TIME=TIME+DT
216. =            PT=RHX*V**2.0/32.2
217. =        102 FORMAT(8(E13.6,2X))
218. =            PRINT 102,TIME,THETA,XHITE,GAMMAD,QCONT,QFM,V,PT
219. =            ZZZ=ABS(THETA)
220. =            IF(THETA)57,57,58
221. =         57 IF(ZZZ-20.1)87,87,88
222. =         87 THETA=THETA+2.0
223. =            GO TO 89
224. =         88 THETA=THETA+20.0
225. =            GO TO 89
226. =         58 IF(ZZZ-19.9)87,87,88
227. =         89 CONTINUE
228. =            T1=T2
229. =            JJ=JJ+1
230. =            IF(THETA-181.0)150,150,192
231. =        192 DRSUBA=-(XK1*(1.0/WCDA)*RHY*(1.0/XBETA**0.5)*RSUBA*B/(C/2.0)**0.5)
232. =            RSUBA=RSUBA+DRSUBA
233. =            GO TO 175
234. =            END
235. +READY ;FINISH
```

APPENDIX B

Listing of FORTRAN Source Deck
and Input Data of Computer Code HRS017
(Version 3)

```
SPAHR,                                    H R SPAHR BOX 651
ACCOUNT,E08666,D09513,G7600,A0049131,RP,KUNC.
FUN(S)
LGO.
'
      PROGRAM HRS017(INPUT,OUTPUT,PUNCH)
C     (WRITTEN BY HAROLD R. SPAHR, DIVISION 9513, SANDIA CORPORATION,
C     SANDIA BASE, ALBUQUERQUE, NEW MEXICO - PHONE 264-1040, BUILDING
C     892, ROOM 233, HOME PHONE 299-5465)
C     THIS IS VERSION THREE OF HRS017. THIS VERSION IS OPERATIONAL ON
C     THE SANDIA CORPORATION CDC 3600.
      DIMENSION ALT(500),RHO(500),AID(11),AIDD(11)
      IREV = 1
      PRINT 700
  700 FORMAT( 1H1 , ////    )
      KJI = 4
      IJK = 0
      IJKL=0
      XK1 = 6.2832**0.5
      III = 0
      XMU = 1.4098E+16
      IRSUBE = 20925697
      RSUBE = IRSUBE
  189 READ 8,(AID(I), I = 1,11)
      READ 7, I1
    7 FORMAT(7X,I3)
      READ 4, (ALT(J),RHO(J), J = 1,I1)
    4 FORMAT(F9.0,7X,E10.3)
  188 READ 8,(AIDD(I), I = 1,11)
    8 FORMAT(11A6)
      READ 100, WCDA
      READ 100, XHITFP
  100 FORMAT(F15.1)
      READ 106, RSUBA
  106 FORMAT(E12.3)
      READ 100, FUDGEC
      READ 100, FUDGEF
      TIME = 0.0
      L = 1
  110 IF ( XHITEP - ALT(L)) 123,122,121
  122 RHX = RHO(L)
      M = L - 1
      ALTD = ALT(M) - ALT(L)
      RATIO = RHO(M)/RHO(L)
      ALOGR = ALOG(RATIO)
      XBETA = ALOGR/(-ALTD)
      GO TO 124
  121 M = L - 1
      IF ( XHITEP - ALT(M)) 181,182,183
  183 L = L - 1
      GO TO 121
  182 RHX = RHO(M)
      ALTD = ALT(M) - ALT(L)
      RATIO = RHO(M)/RHO(L)
```

```
      ALOGR = ALOG(RATIO)
      XBETA = ALOGR/(-ALTD)
      GO TO 124
  181 ALTD = ALT(M) - ALT(L)
      RATIO = RHO(M)/RHO(L)
      ALOGR = ALOG(RATIO)
      XBETA = ALOGR/(-ALTD)
      POWER = (-XBETA*ALT(L))
      RHOSS = RHO(L)/(EXP(POWER))
      POWER2 = (-XBETA*XHITEP)
      RHX = RHOSS*EXP(POWER2)
      GO TO 124
  123 L = L + 1
      GO TO 110
  124 CONTINUE
      RHY = RHX
  175 CONTINUE
      IF ( KJI - 60 ) 913,912,912
  912 KJI = 4
      PRINT 700
  913 CONTINUE
      PRINT 701, IREV
  701 FORMAT( ///    , 53X , 12H REVOLUTION , I3   )
      KJI= KJI + 4
      IF ( KJI - 61 ) 915,914,914
  914 KJI = 4
      PRINT 700
  915 CONTINUE
      PRINT 916
  916 FORMAT(    //    )
      KJI = KJI + 3
      IF ( KJI - 59 ) 918,917,917
  917 KJI = 4
      PRINT 700
  918 CONTINUE
      PRINT 702
  702 FORMAT( 9X , 6H TIME , 6X , 7H THETA , 6X , 10H ALTITUDE , 7X , 7H
     1 GAMMA , 7X , 7H QCONT , 8X , 5H QFM , 4X , 10H VELOCITY , 11X, 3H
     2 P , /  ,111X , 3H T    )
      KJI = KJI + 2
      IF ( KJI - 60 ) 920,919,919
  919 KJI = 4
      PRINT 700
  920 CONTINUE
      PRINT 916
      KJI = KJI + 3
      THETA = -180.0
      JJ = 0
  150 CONTINUE
      RSUBP = RSUBF + XHITEP
      B = RSUBA + RSUBP
      C = RSUBA - RSUBP
      D = THETA/57.29578
      E = COS(D)
```

```
      F = 2.0*RSUBA/( B + C*E )
      R = RSUBP*F
      XHITE = R - RSUBE
   77 IF ( XHITE ) 188,15,15
   15 CONTINUE
   60 IF ( XHITE - ALT(L)) 73,72,71
   72 RHX = RHO(L)
      GO TO 74
   71 M = L - 1
      IF ( M - 1 ) 161,161,162
  161 RHX = 0.0
      GO TO 74
  162 IF ( XHITE - ALT(M)) 171,172,173
  173 L = L - 1
      GO TO 71
  172 RHX = RHO(M)
      GO TO 74
  171 ALTD = ALT(M) - ALT(L)
      RATIO = RHO(M)/RHO(L)
      ALOGR = ALOG(RATIO)
      BETA = ALOGR/(-ALTD)
      POWER = (-BETA*ALT(L))
      RHOSS = RHO(L)/(EXP(POWER))
      POWER2 = (-BETA*XHITE)
      RHX = RHOSS*EXP(POWER2)
      GO TO 74
   73 L = L + 1
      GO TO 60
   74 CONTINUE
      X = RSUBP/( RSUBA + RSUBP - R )
      Y = RSUBA/R
      Z = (0.999999)*(( X*Y )**0.5)
      GAMMA = ACOSF( Z )
      GAMMAD = GAMMA*57.29578
      AAA = B/2.0
      XN = 1.0/(((AAA**3.0)/XMU)**0.5)
      V = (XMU*((2.0/R) - (1.0/AAA)))**0.5
      QCONT = 865.0*((RHX/0.076474)**0.5)*((V/10000.0)**3.15)
      QFM = (RHX*(V**3.0))/50063.0
      EE = C/B
      EEE = ACOSF( 0.999999*(( AAA - R )/( AAA*EE )))
      T2 = ( EEE - EE*SIN(EFE))/XN
      DT = ABS( T2 - T1 )
      IF ( JJ ) 133, 133, 134
  133 DT = 0
  134 CONTINUE
      TIME = TIME + DT
      PT = RHX*(V**2.0)/32.2
      PTA = PT/2116.4
      XHR = ( V**2.0 )/50063.0
      QDOT1= FUDGEC*QCONT
      QDOT2 = FUDGEF*QFM
      IF ( KJI - 62 ) 911,910,910
  910 KJI = 4
```

```
      PRINT 700
  911 CONTINUE
      PRINT 102, TIME, THETA, XHITE, GAMMAD, QDOT1, QDOT2, V, PT
  102 FORMAT( 6X, F10.1, 4X , F7.2,  4X,  F13.2,  4X , F10.5,  4X,   F9.
     12,  4X , F10.3,  4X , F9.2 , 4X , F13.5 )
      KJI = KJI + 1
      IF(QDOT1-QDOT2)632,632,633
  632 QDOT = QDOT1
      GO TO 634
  633 QDOT = QDOT2
  634 CONTINUE
      QDOTHR = QDOT/XHR
      RDOT = 0.0
      IF ( IJKL ) 401,401,402
  401 DT = 0.0
  402 CONTINUE
      XTIME = XTIME + DT
      IJKL = IJKL + 1
      IF ( XHITE - 1000000.0 ) 213,213,214
  213 CONTINUE
      IF ( IJK - 995 ) 262,262,263
  262 CONTINUE
      IJK = IJK + 1
   81 FORMAT(1X,F9.4,1X,F9.3,1X,F9.4,1X,F9.7,1X,F9.6,11X,2A6)
      PUNCH 81,XTIME, XHR, RDOT, QDOTHR, PTA,(AIDD(I), I = 1,2)
  263 CONTINUE
      GO TO 215
  214 CONTINUE
      IJKL = 0
      XTIME = 0.0
  215 CONTINUE
      ZZZ = ABS(THETA)
      IF ( THETA ) 57, 57, 58
   57 IF ( ZZZ - 20.1 ) 87, 87, 88
   87 THETA = THETA + 2.0
      GO TO 89
   88 THETA = THETA + 20.0
      GO TO 89
   58 IF ( ZZZ - 19.9 ) 87, 87, 88
   89 CONTINUE
      T1 = T2
      JJ = JJ + 1
      IF ( THETA - 181.0 ) 150,150,192
  192 DRSUBA=-(XK1*(1.0/WCDA)*RHY*(1.0/XBETA**0.5)*RSUBA*B/(C/2.0)**0.5)
      RSUBA = RSUBA + DRSUBA
      IREV = IREV + 1
      GO TO 175
      END
```

```
                U. S. STANDARD ATMOSPHERE, 1962
      257          NUMBER OF VALUES OF ALT AND RH
  2320000         8.895E-15
  2300000         9.491E-15
  2280000         1.013E-14
```

2260000	1.081E-14
2240000	1.155E-14
2220000	1.234E-14
2200000	1.318E-14
2180000	1.409E-14
2160000	1.506E-14
2140000	1.611E-14
2120000	1.723E-14
2100000	1.843E-14
2080000	1.973E-14
2060000	2.112E-14
2040000	2.262E-14
2020000	2.423E-14
2000000	2.596E-14
1980000	2.783E-14
1960000	2.985E-14
1940000	3.207E-14
1920000	3.446E-14
1900000	3.704E-14
1880000	3.983E-14
1860000	4.286E-14
1840000	4.613E-14
1820000	4.967E-14
1800000	5.351E-14
1780000	5.767E-14
1760000	6.218E-14
1740000	6.707E-14
1720000	7.237E-14
1700000	7.814E-14
1680000	8.440E-14
1660000	9.120E-14
1640000	9.861E-14
1620000	1.069E-13
1600000	1.160E-13
1580000	1.259E-13
1560000	1.368E-13
1540000	1.487E-13
1520000	1.618E-13
1500000	1.761E-13
1480000	1.919E-13
1460000	2.092E-13
1440000	2.283E-13
1420000	2.493E-13
1400000	2.724E-13
1380000	2.979E-13
1360000	3.261E-13
1340000	3.572E-13
1320000	3.915E-13
1300000	4.301E-13
1280000	4.734E-13
1260000	5.215E-13
1240000	5.752E-13
1220000	6.351E-13
1200000	7.020E-13

1180000		7.769E-13	
1160000		8.607E-13	
1140000		9.548E-13	
1120000		1.060E-12	
1100000		1.179E-12	
1080000		1.313E-12	
1060000		1.464E-12	
1040000		1.634E-12	
1020000		1.827E-12	
1000000	249600	2.046E-12	5.1286E-9
980000	249143	2.294E-12	5.6872E-9
960000	248431	2.583E-12	6.3160E-9
940000	247695	2.912E-12	7.0257E-9
920000	246934	3.290E-12	7.8283E-9
900000	246138	3.724E-12	8.7375E-9
880000	245318	4.224E-12	9.7696E-9
860000	244468	4.800E-12	1.0943E-8
840000	243590	5.466E-12	1.2281E-8
820000	242682	6.238E-12	1.3809E-8
800000	241739	7.135E-12	1.5558E-8
780000	240767	8.179E-12	1.7565E-8
760000	239765	9.398E-12	1.9872E-8
740000	238385	1.086E-11	2.2534E-8
720000	236834	1.260E-11	2.5624E-8
700000	235238	1.467E-11	2.9221E-8
680000		1.713E-11	
660000	231919	2.008E-11	3.8351E-8
640000	230191	2.363E-11	4.4148E-8
620000	228246	2.796E-11	5.0998E-8
600000	225369	3.350E-11	5.9175E-8
580000	222423	4.040E-11	6.9023E-8
560000	219462	4.906E-11	8.0964E-8
540000	214415	6.090E-11	9.5641E-8
520000	208626	7.720E-11	1.1405E-7
500000	200259	1.020E-10	1.3799E-7
490000	195555	1.188E-10	1.5282E-7
480000	189443	1.415E-10	1.7033E-7
470000	183099	1.706E-10	.19134E-7
460000	176510	2.088E-10	2.1689E-7
450000	169645	2.600E-10	2.4846E-7
440000	162467	3.301E-10	2.8819E-7
430000	154930	4.294E-10	3.3931E-7
420000	146951	5.751E-10	4.0686E-7
410000	138452	7.990E-10	4.9911E-7
400000	129310	1.1640E-9	6.3049E-7
390000	121336	1.7430E-9	8.2674E-7
380000	116244	2.5790E-9	1.1167E-6
370000	110838	3.9710E-9	1.5552E-6
360000	105349	6.3850E-9	2.2481E-6
350000	102423	1.0120E-8	3.3543E-6
340000	99344	1.6540E-8	5.1376E-6
330000	96103	2.7960E-8	8.1073E-6
320000	94228	4.7740E-8	1.3176E-5
310000	91753	8.3140E-8	2.1913E-5

300000	89450	1.4880E-7	3.7368E-5
290000	88400	2.6600E-7	6.5244E-5
280000	88400	4.6610E-7	1.1433E-4
270000	88400	8.1720E-7	2.0046E-4
260000	89110	1.4090E-6	3.5127E-4
250000	91950	2.2630E-6	6.0065E-4
240000	94712	3.5353E-6	9.9546E-4
230000	97396	5.3888E-6	1.6046E-3
220000	100011	8.0356E-6	2.5229E-3
210000	102562	1.1748E-5	3.8790E-3
200000	104798	1.6957E-5	5.8458E-3
195000	105413	2.0472E-5	7.1405E-3
190000	106025	2.4663E-5	8.7026E-3
185000	106634	2.9651E-5	1.0583E-2
180000	107240	3.5578E-5	1.2843E-2
175000	107843	4.2605E-5	1.5554E-2
170000	108202	5.1159E-5	1.8801E-2
165000	108202	6.1822E-5	2.2719E-2
160000	108202	7.4713E-5	2.7457E-2
155000	108143	9.0400E-5	3.3186E-2
150000	107299	1.1119E-4	4.0182E-2
145000	106447	1.3722E-4	4.8805E-2
140000	105588	1.6994E-4	5.9471E-2
135000	104722	2.1122E-4	7.2712E-2
130000	103848	2.6353E-4	8.9210E-2
125000	102967	3.3006E-4	1.0984E-1
120000	102077	4.1506E-4	1.3575E-1
115000	101179	5.2412E-4	1.6842E-1
110000	100272	6.6470E-4	2.0978E-1
105000	99418	8.4570E-4	2.6238E-1
101800	99208	9.8152E-4	3.0324E-1
101000	99155	1.0189E-3	3.1444E-1
100000	99090	1.0676E-3	3.2905E-1
99000	99024	1.1188E-3	3.4435E-1
98000	98958	1.1725E-3	3.6040E-1
97000	98892	1.2288E-3	3.7721E-1
96000	98826	1.2879E-3	3.9484E-1
95200	98773	1.3373E-3	4.0955E-1
95000	98759	1.3500E-3	4.1331E-1
94000	98693	1.4152E-3	4.3268E-1
93000	98627	1.4836E-3	4.5299E-1
92000	98561	1.5554E-3	4.7428E-1
91000	98494	1.6308E-3	4.9660E-1
90000	98428	1.7100E-3	5.2001E-1
89000	98362	1.7931E-3	5.4456E-1
88600	98335	1.8275E-3	5.5471E-1
88000	98295	1.8804E-3	5.7031E-1
87000	98229	1.9721E-3	5.9731E-1
86000	98162	2.0685E-3	6.2563E-1
85000	98095	2.1696E-3	6.5534E-1
84000	98029	2.2759E-3	6.8651E-1
83000	97962	2.3876E-3	7.1921E-1
82000	97895	2.5049E-3	7.5352E-1
81000	97828	2.6281E-3	7.8952E-1

80000	97762	2.7576E-3	8.2730E-1
79000	97695	2.8937E-3	8.6694E-1
78000	97628	3.0368E-3	9.0854E-1
77000	97561	3.1871E-3	9.5221E-1
76000	97493	3.3451E-3	9.9804E-1
75400	97453	3.4438E-3	1.0266E+0
75000	97426	3.5112E-3	1.0462E+0
74000	97359	3.6858E-3	1.0967E+0
73000	97292	3.8694E-3	1.1497E+0
72000	97224	4.0624E-3	1.2054E+0
71000	97157	4.2653E-3	1.2638E+0
70000	97090	4.4787E-3	1.3252E+0
69000	97022	4.7031E-3	1.3897E+0
68800	97009	4.7494E-3	1.4030E+0
68000	96955	4.9391E-3	1.4574E+0
67000	96887	5.1874E-3	1.5285E+0
66000	96819	5.4485E-3	1.6032E+0
65000	96808	5.7164E-3	1.6816E+0
64000	96808	5.9961E-3	1.7639E+0
63000	96808	6.2895E-3	1.8502E+0
62400	96808	6.4724E-3	1.9040E+0
62000	96808	6.5973E-3	1.9408E+0
61000	96808	6.9202E-3	2.0357E+0
60000	96808	7.2589E-3	2.1354E+0
59000	96808	7.6142E-3	2.2399E+0
58000	96808	7.9870E-3	2.3496E+0
57000	96808	8.3780E-3	2.4646E+0
56000	96808	8.7882E-3	2.5853E+0
55800	96808	8.8727E-3	2.6101E+0
55000	96808	9.2186E-3	2.7119E+0
54000	96808	9.6701E-3	2.8447E+0
53000	96808	1.0144E-2	2.9840E+0
52000	96808	1.0641E-2	3.1302E+0
51000	96808	1.1162E-2	3.2835E+0
50000	96808	1.1709E-2	3.4444E+0
49200	96808	1.2165E-2	3.5788E+0
49000	96808	1.2282E-2	3.6132E+0
48000	96808	1.2884E-2	3.7902E+0
47000	96808	1.3516E-2	3.9760E+0
46000	96808	1.4178E-2	4.4074E+0
45000	96808	1.4873E-2	4.3753E+0
44000	96808	1.5602E-2	4.5898E+0
43000	96808	1.6367E-2	4.8148E+0
42600	96808	1.6684E-2	4.9079E+0
42000	96808	1.7170E-2	5.0509E+0
41000	96808	1.8012E-2	5.2986E+0
40000	96808	1.8895E-2	5.5584E+0
39000	96808	1.9822E-2	5.8311E+0
38000	96808	2.0794E-2	6.1171E+0
37000	96808	2.1814E-2	6.4172E+0
36000	96874	2.2853E-2	6.7320E+0
35000	97314	2.3751E-2	7.0603E+0
34000	97752	2.4676E-2	7.4015E+0
33000	98188	2.5629E-2	7.7559E+0

```
   32000   98622 2.6610E-2 8.1241E+0
   31000   99055 2.7619E-2 8.5062E+0
   30000   99485 2.8657E-2 8.9029E+0
   29500   99699 2.9187E-2 9.1068E+0
   29000   99914 2.9725E-2 9.3144E+0
   28000  100340 3.0823E-2 9.7413E+0
   27000  100765 3.1952E-2 1.0184E+1
   26000  101189 3.3113E-2 1.0643E+1
   25000  101610 3.4306E-2 1.1118E+1
   24000  102030 3.5531E-2 1.1611E+1
   23000  102448 3.6790E-2 1.2121E+1
   22000  102865 3.8083E-2 1.2649E+1
   21000  103280 3.9410E-2 1.3196E+1
   20000  103693 4.0773E-2 1.3761E+1
   19000  104105 4.2171E-2 1.4346E+1
   18000  104515 4.3606E-2 1.4952E+1
   17000  104923 4.5079E-2 1.5578E+1
   16400  105168 4.5980E-2 1.5963E+1
   16000  105330 4.6589E-2 1.6224E+1
   15000  105736 4.8137E-2 1.6893E+1
   14000  106139 4.9725E-2 1.7584E+1
   13000  106542 5.1353E-2 1.8298E+1
   12000  106943 5.3022E-2 1.9034E+1
   11000  107342 5.4731E-2 1.9795E+1
   10000  107740 5.6483E-2 2.0581E+1
    9800  107820 5.6839E-2 2.0741E+1
    9000  108137 5.8278E-2 2.1391E+1
    8000  108532 6.0116E-2 2.2228E+1
    7000  108926 6.1998E-2 2.3090E+1
    6600  109083 6.2763E-2 2.3443E+1
    6000  109319 6.3925E-2 2.3980E+1
    5000  109710 6.5898E-2 2.4897E+1
    4000  110099 6.7917E-2 2.5843E+1
    3300  110371 6.9359E-2 2.6522E+1
    3000  110488 6.9984E-2 2.6817E+1
    2000  110875 7.2098E-2 2.7821E+1
    1000  111261 7.4262E-2 2.8856E+1
       0  111645 7.6474E-2 2.9921E+1
GLFC CONT.
  27.008
  260000.0
  1.2673E+9
 1.225
 1.000
```

APPENDIX C

Trajectory and Reentry Environment
Output From Computer Code HRS017 (Version 3)
for a Perigee Altitude of 260,000 Feet
(Five Revolutions)

Part 1. Trajectory and Reentry Environment Tabulated Data (59)

Part 2. Listing of Punched Card CMA Input (64)

Part 1

Trajectory and Reentry Environment Tabulated Data

REVOLUTION 1

TIME	THETA	ALTITUDE	GAMMA	QCONT	QFM	VELOCITY	P/T
0.0	-180.00	1246374303.00	.08103	0.00	0.000	604.83	0.00000
385031.7	-160.00	435989528.61	74.58411	0.00	0.000	6310.82	0.00000
422284.5	-140.00	139889450.89	67.37027	0.00	0.000	12387.44	0.00000
428399.5	-120.00	59770068.80	58.34150	0.00	0.000	18097.74	0.00000
430259.2	-100.00	29160354.42	48.85871	0.00	0.000	23260.87	0.00000
431073.2	-80.00	14756604.58	39.19641	0.00	0.000	27718.45	0.00000
431527.3	-60.00	7165364.31	29.44712	0.00	0.000	31334.53	0.00000
431831.2	-40.00	3013545.18	19.65155	0.00	0.000	33999.00	0.00000
432067.0	-20.00	907340.93	9.83144	.40	.003	35630.81	.00014
432088.6	-18.00	782353.05	8.84866	.60	.007	35735.00	.00032
432109.9	-16.00	671322.89	7.86580	.91	.017	35828.31	.00073
432131.0	-14.00	573978.04	6.88287	1.41	.040	35910.70	.00172
432152.0	-12.00	490081.36	5.89988	2.36	.110	35982.17	.00477
432172.7	-10.00	419429.69	4.91687	5.26	.548	36042.67	.02364
432193.4	-8.00	361852.84	3.93386	16.70	5.491	36092.20	.23655
432213.9	-6.00	317212.74	2.95091	51.73	52.499	36130.74	2.25909
432234.3	-4.00	285402.70	1.96822	128.88	325.070	36158.28	13.97752
432254.2	-2.00	266346.90	.98661	219.66	942.879	36174.80	40.52385
432269.3	0.00	260000.00	.08103	261.24	1332.941	36180.31	57.27956
432284.3	2.00	266346.90	.98661	219.66	942.879	36174.80	40.52385
432304.3	4.00	285402.70	1.96822	128.88	325.070	36158.28	13.97752
432324.6	6.00	317212.74	2.95091	51.73	52.499	36130.74	2.25909
432345.1	8.00	361852.84	3.93386	16.70	5.491	36092.20	.23655
432365.8	10.00	419429.69	4.91687	5.26	.548	36042.67	.02364
432386.5	12.00	490081.36	5.89988	2.36	.110	35982.17	.00477
432407.5	14.00	573978.04	6.88287	1.41	.040	35910.70	.00172
432428.6	16.00	671322.89	7.86580	.91	.017	35828.31	.00073
432450.0	18.00	782353.05	8.84866	.60	.007	35735.00	.00032
432471.5	20.00	907340.93	9.83144	.40	.003	35630.81	.00014
432707.3	40.00	3013545.18	19.65155	0.00	0.000	33999.00	0.00000
433011.2	60.00	7165364.31	29.44712	0.00	0.000	31334.53	0.00000
433465.4	80.00	14756604.58	39.19641	0.00	0.000	27718.45	0.00000
434279.3	100.00	29160354.42	48.85871	0.00	0.000	23260.87	0.00000
436139.0	120.00	59770068.80	58.34150	0.00	0.000	18097.74	0.00000
442254.0	140.00	139889450.89	67.37027	0.00	0.000	12387.44	0.00000
479506.8	160.00	435989528.61	74.58411	0.00	0.000	6310.82	0.00000
864538.5	180.00	1246374303.00	.08103	0.00	0.000	604.83	0.00000

REVOLUTION 2

TIME	THETA	ALTITUDE	GAMMA	QCONT	QFM	VELOCITY	P_T
864538.5	-180.00	87317213.87	.08103	0.00	0.000	6529.81	0.00000
869882.6	-160.00	75383630.38	32.01571	0.00	0.000	8655.35	0.00000
873458.9	-140.00	52177305.96	41.73109	0.00	0.000	12955.79	0.00000
875416.7	-120.00	32466653.44	41.27324	0.00	0.000	17613.65	0.00000
876481.1	-100.00	19196353.25	36.87035	0.00	0.000	22020.58	0.00000
877109.9	-80.00	10804029.68	30.67357	0.00	0.000	25899.43	0.00000
877523.9	-60.00	5591861.18	23.55299	0.00	0.000	29076.55	0.00000
877828.3	-40.00	2460203.00	15.92547	0.00	0.000	31429.83	0.00000
878077.2	-20.00	786563.55	8.02384	.46	.006	32875.09	.00026
878100.3	-18.00	685349.55	7.22488	.67	.012	32967.46	.00055
878123.3	-16.00	595256.66	6.42486	.98	.025	33050.19	.00119
878146.1	-14.00	516127.36	5.62392	1.50	.059	33123.26	.00278
878168.7	-12.00	447823.74	4.82219	2.77	.200	33186.63	.00937
878191.2	-10.00	390227.13	4.01980	7.00	1.267	33240.29	.05926
878213.6	-8.00	343237.70	3.21690	20.10	10.391	33284.22	.48538
878235.9	-6.00	306774.18	2.41367	53.77	74.113	33318.41	3.45835
878258.1	-4.00	280773.61	1.61044	113.68	330.464	33342.83	15.40931
878280.2	-2.00	265191.17	.80833	175.59	787.336	33357.49	36.69677
878300.5	0.00	260000.00	.08103	202.35	1045.117	33362.38	48.70450
878320.7	2.00	265191.17	.80833	175.59	787.336	33357.49	36.69677
878342.9	4.00	280773.61	1.61044	113.68	330.464	33342.83	15.40931
878365.1	6.00	306774.18	2.41367	53.77	74.113	33318.41	3.45835
878387.4	8.00	343237.70	3.21690	20.10	10.391	33284.22	.48538
878409.8	10.00	390227.13	4.01980	7.00	1.267	33240.29	.05926
878432.2	12.00	447823.74	4.82219	2.77	.200	33186.63	.00937
878454.9	14.00	516127.36	5.62392	1.50	.059	33123.26	.00278
878477.7	16.00	595256.66	6.42486	.98	.025	33050.19	.00119
878500.6	18.00	685349.55	7.22488	.67	.012	32967.46	.00055
878523.8	20.00	786563.55	8.02384	.46	.006	32875.09	.00026
878772.7	40.00	2460203.00	15.92547	0.00	0.000	31429.83	0.00000
879077.1	60.00	5591861.18	23.55299	0.00	0.000	29076.55	0.00000
879491.1	80.00	10804029.68	30.67357	0.00	0.000	25899.43	0.00000
880119.8	100.00	19196353.25	36.87035	0.00	0.000	22020.58	0.00000
881184.3	120.00	32466653.44	41.27324	0.00	0.000	17613.65	0.00000
883142.1	140.00	52177305.96	41.73109	0.00	0.000	12955.79	0.00000
886718.4	160.00	75383630.38	32.01571	0.00	0.000	8655.35	0.00000
892062.4	180.00	87317213.87	.08103	0.00	0.000	6529.81	0.00000

REVOLUTION 3

TIME	THETA	ALTITUDE	GAMMA	QCONT	QFM	VELOCITY	P/T
892062.4	-180.00	49694329.15	.08103	0.00	0.000	9598.79	0.00000
894511.1	-160.00	45052123.54	20.44569	0.00	0.000	10964.89	0.00000
896429.5	-140.00	34551588.47	30.50369	0.00	0.000	14181.58	0.00000
897717.5	-120.00	23676079.84	32.54336	0.00	0.000	18029.01	0.00000
898547.1	-100.00	15029764.23	30.32707	0.00	0.000	21841.83	0.00000
899099.0	-80.00	8880775.63	25.87083	0.00	0.000	25275.33	0.00000
899491.9	-60.00	4753969.90	20.17387	0.00	0.000	28122.28	0.00000
899795.5	-40.00	2149512.58	13.76882	.02	.000	30245.51	.00000
900051.0	-20.00	716824.17	6.97250	.51	.008	31554.38	.00040
900075.0	-18.00	629243.17	6.28018	.73	.016	31638.15	.00080
900098.8	-16.00	551194.25	5.58633	1.07	.034	31713.19	.00169
900122.5	-14.00	482572.38	4.89114	1.70	.087	31779.46	.00424
900146.0	-12.00	423285.29	4.19480	3.36	.337	31836.96	.01645
900169.4	-10.00	373253.33	3.49749	8.68	2.235	31885.64	.10896
900192.8	-8.00	332409.30	2.79941	23.29	16.014	31925.50	.77987
900216.0	-6.00	300698.40	2.10083	56.26	93.134	31956.52	4.53118
900239.1	-4.00	278078.08	1.40213	107.49	339.164	31978.69	16.48961
900262.3	-2.00	264518.01	.70465	156.78	720.493	31991.99	35.01462
900283.7	0.00	260000.00	.08103	177.39	921.931	31996.42	44.79793
900305.2	2.00	264518.01	.70465	156.78	720.493	31991.99	35.01462
900328.3	4.00	278078.08	1.40213	107.49	339.164	31978.69	16.48961
900351.5	6.00	300698.40	2.10083	56.26	93.134	31956.52	4.53118
900374.7	8.00	332409.30	2.79941	23.29	16.014	31925.50	.77987
900398.0	10.00	373253.33	3.49749	8.68	2.235	31885.64	.10896
900421.4	12.00	423285.29	4.19480	3.36	.337	31836.96	.01645
900444.9	14.00	482572.38	4.89114	1.70	.087	31779.46	.00424
900468.6	16.00	551194.25	5.58633	1.07	.034	31713.19	.00169
900492.5	18.00	629243.17	6.28018	.73	.016	31638.15	.00080
900516.5	20.00	716824.17	6.97250	.51	.008	31554.38	.00040
900772.0	40.00	2149512.58	13.76882	.02	.000	30245.51	.00000
901075.5	60.00	4753969.90	20.17387	0.00	0.000	28122.28	0.00000
901468.5	80.00	8880775.63	25.87083	0.00	0.000	25275.33	0.00000
902020.3	100.00	15029764.23	30.32707	0.00	0.000	21841.83	0.00000
902850.0	120.00	23676079.84	32.54336	0.00	0.000	18029.01	0.00000
904137.9	140.00	34551588.47	30.50369	0.00	0.000	14181.58	0.00000
906056.3	160.00	45052123.54	20.44569	0.00	0.000	10964.89	0.00000
908505.0	180.00	49694329.15	.08103	0.00	0.000	9598.79	0.00000

REVOLUTION 4

TIME	THETA	ALTITUDE	GAMMA	QCONT	QFM	VELOCITY	P_T
908505.0	-180.00	26589219.24	.08103	0.00	0.000	13527.57	0.00000
909698.0	-160.00	24872938.68	11.57725	0.00	0.000	14325.96	0.00000
910740.2	-140.00	20558352.14	19.22514	0.00	0.000	16409.28	0.00000
911562.3	-120.00	15325979.23	22.32204	0.00	0.000	19166.80	0.00000
912182.3	-100.00	10468617.96	22.01518	0.00	0.000	22084.07	0.00000
912650.8	-80.00	6550771.55	19.48767	0.00	0.000	24814.69	0.00000
913016.9	-60.00	3666836.45	15.56422	0.00	0.000	27131.32	0.00000
913318.2	-40.00	1728449.73	10.78241	.03	.000	28882.70	.00000
913582.0	-20.00	620005.49	5.50526	.64	.015	29970.68	.00078
913607.1	-18.00	551236.06	4.96116	.90	.029	30040.50	.00151
913632.1	-16.00	489851.75	4.41507	1.35	.065	30103.07	.00335
913656.9	-14.00	435803.98	3.86723	2.38	.202	30158.35	.01041
913681.6	-12.00	389049.79	3.31788	5.30	.996	30206.32	.05126
913706.3	-10.00	349551.87	2.76727	12.73	5.718	30246.94	.29393
913730.8	-8.00	317278.60	2.21566	29.60	30.790	30280.21	1.58092
913755.3	-6.00	292204.07	1.66337	60.93	130.122	30306.10	6.67547
913779.7	-4.00	274308.11	1.11092	101.09	357.391	30324.60	18.32355
913804.1	-2.00	263576.31	.55998	136.05	646.617	30335.70	33.14012
913827.0	0.00	260000.00	.08103	150.03	785.987	30339.40	40.27812
913850.0	2.00	263576.31	.55998	136.05	646.617	30335.70	33.14012
913874.3	4.00	274308.11	1.11092	101.09	357.391	30324.60	18.32355
913898.8	6.00	292204.07	1.66337	60.93	130.122	30306.10	6.67547
913923.2	8.00	317278.60	2.21566	29.60	30.790	30280.21	1.58092
913947.8	10.00	349551.87	2.76727	12.73	5.718	30246.94	.29393
913972.4	12.00	389049.79	3.31788	5.30	.996	30206.32	.05126
913997.1	14.00	435803.98	3.86723	2.38	.202	30158.35	.01041
914022.0	16.00	489851.75	4.41507	1.35	.065	30103.07	.00335
914046.9	18.00	551236.06	4.96116	.90	.029	30040.50	.00151
914072.1	20.00	620005.49	5.50526	.64	.015	29970.68	.00078
914335.8	40.00	1728449.73	10.78241	.03	.000	28882.70	.00000
914637.1	60.00	3666836.45	15.56422	0.00	0.000	27131.32	0.00000
915003.2	80.00	6550771.55	19.48767	0.00	0.000	24814.69	0.00000
915471.7	100.00	10468617.96	22.01518	0.00	0.000	22084.07	0.00000
916091.7	120.00	15325979.23	22.32204	0.00	0.000	19166.80	0.00000
916913.8	140.00	20558352.14	19.22514	0.00	0.000	16409.28	0.00000
917956.0	160.00	24872938.68	11.57725	0.00	0.000	14325.96	0.00000
919149.0	180.00	26589219.24	.08103	0.00	0.000	13527.57	0.00000

REVOLUTION 5

TIME	THETA	ALTITUDE	GAMMA	QCONT	QFM	VELOCITY	P/T
919149.0	-180.00	10648925.41	.08103	0.00	0.000	18936.18	0.00000
919723.5	-160.00	10188847.03	4.72471	0.00	0.000	19281.68	0.00000
920268.2	-140.00	8935972.78	8.47809	0.00	0.000	20243.61	0.00000
920759.9	-120.00	7200796.56	10.71125	0.00	0.000	21634.57	0.00000
921191.7	-100.00	5329363.21	11.35328	0.00	0.000	23227.34	0.00000
921567.5	-80.00	3593262.23	10.62025	0.00	0.000	24810.29	0.00000
921897.6	-60.00	2158865.07	8.82470	.01	.000	26210.79	.00000
922193.8	-40.00	1108055.53	6.27672	.10	.000	27299.38	.00003
922468.3	-20.00	472298.05	3.25368	1.25	.072	27987.08	.00398
922495.0	-18.00	431969.38	2.93497	1.99	.179	28031.50	.00995
922521.6	-16.00	395882.16	2.61425	3.67	.607	28071.33	.03364
922548.1	-14.00	364037.92	2.29175	7.21	2.338	28106.54	.12931
922574.5	-12.00	336437.85	1.96773	14.08	8.873	28137.10	.49029
922600.8	-10.00	313082.83	1.64245	26.46	31.265	28163.00	1.72599
922627.1	-8.00	293973.49	1.31621	46.05	94.437	28184.22	5.20949
922653.4	-6.00	279110.28	.98939	70.28	219.502	28200.74	12.10152
922679.6	-4.00	268493.52	.66273	94.68	397.905	28212.55	21.92794
922705.8	-2.00	262123.39	.33882	112.71	563.394	28219.63	31.04004
922730.8	0.00	260000.00	.08103	119.45	632.641	28222.00	34.85223
922755.7	2.00	262123.39	.33882	112.71	563.394	28219.63	31.04004
922781.9	4.00	268493.52	.66273	94.68	397.905	28212.55	21.92794
922808.2	6.00	279110.28	.98939	70.28	219.502	28200.74	12.10152
922834.4	8.00	293973.49	1.31621	46.05	94.437	28184.22	5.20949
922860.7	10.00	313082.83	1.64245	26.46	31.265	28163.00	1.72599
922887.1	12.00	336437.85	1.96773	14.08	8.873	28137.10	.49029
922913.5	14.00	364037.92	2.29175	7.21	2.338	28106.54	.12931
922940.0	16.00	395882.16	2.61425	3.67	.607	28071.33	.03364
922966.6	18.00	431969.38	2.93497	1.99	.179	28031.50	.00995
922993.3	20.00	472298.05	3.25368	1.25	.072	27987.08	.00398
923267.7	40.00	1108055.53	6.27672	.10	.000	27299.38	.00003
923564.0	60.00	2158865.07	8.82470	.01	.000	26210.79	.00000
923894.0	80.00	3593262.23	10.62025	0.00	0.000	24810.29	0.00000
924269.9	100.00	5329363.21	11.35328	0.00	0.000	23227.34	0.00000
924701.6	120.00	7200796.56	10.71125	0.00	0.000	21634.57	0.00000
925193.4	140.00	8935972.78	8.47809	0.00	0.000	20243.61	0.00000
925738.1	160.00	10188847.03	4.72471	0.00	0.000	19281.68	0.00000
926312.5	180.00	10648925.41	.08103	0.00	0.000	18936.18	0.00000

Part 2

Listing of Punched Card CMA Input

REVOLUTION 1

TIME	H_R	QDOTR	$QDOTC/H_R$	P_{TA}	I. D.
0.0000	25359.133	0.0000	.0000001	.000000	GLFC CONT.
21.5707	25507.659	0.0000	.0000003	.000000	GLFC CONT.
42.9054	25641.041	0.0000	.0000007	.000000	GLFC CONT.
64.0311	25759.116	0.0000	.0000015	.000001	GLFC CONT.
84.9734	25861.740	0.0000	.0000043	.000002	GLFC CONT.
105.7555	25948.789	0.0000	.0000211	.000011	GLFC CONT.
126.3964	26020.155	0.0000	.0002110	.000112	GLFC CONT.
146.9050	26075.753	0.0000	.0019838	.001067	GLFC CONT.
167.2577	26115.514	0.0000	.0049350	.006604	GLFC CONT.
187.2450	26139.390	0.0000	.0084034	.019148	GLFC CONT.
202.2643	26147.352	0.0000	.0099910	.027065	GLFC CONT.
217.2836	26139.390	0.0000	.0084034	.019148	GLFC CONT.
237.2709	26115.514	0.0000	.0049350	.006604	GLFC CONT.
257.6236	26075.753	0.0000	.0019838	.001067	GLFC CONT.
278.1322	26020.155	0.0000	.0002110	.000112	GLFC CONT.
298.7731	25948.789	0.0000	.0000211	.000011	GLFC CONT.
319.5552	25861.740	0.0000	.0000043	.000002	GLFC CONT.
340.4975	25759.116	0.0000	.0000015	.000001	GLFC CONT.
361.6232	25641.041	0.0000	.0000007	.000000	GLFC CONT.
382.9579	25507.659	0.0000	.0000003	.000000	GLFC CONT.
404.5286	25359.133	0.0000	.0000001	.000000	GLFC CONT.

REVOLUTION 2

TIME	H_R	QDOTR	$QDOTC/H_R$	P_{TA}	I. D.
0.0000	21588.225	0.0000	.0000003	.000000	GLFC CONT.
23.1705	21709.712	0.0000	.0000005	.000000	GLFC CONT.
46.1365	21818.811	0.0000	.0000012	.000001	GLFC CONT.
68.9223	21915.391	0.0000	.0000027	.000001	GLFC CONT.
91.5515	21999.332	0.0000	.0000091	.000004	GLFC CONT.
114.0469	22070.534	0.0000	.0000574	.000028	GLFC CONT.
136.4306	22128.908	0.0000	.0004696	.000229	GLFC CONT.
158.7236	22174.384	0.0000	.0024248	.001634	GLFC CONT.
180.9433	22206.906	0.0000	.0051190	.007281	GLFC CONT.
203.0887	22226.436	0.0000	.0079001	.017339	GLFC CONT.
223.3214	22232.948	0.0000	.0091015	.023013	GLFC CONT.
243.5542	22226.436	0.0000	.0079001	.017339	GLFC CONT.
265.6995	22206.906	0.0000	.0051190	.007281	GLFC CONT.
287.9193	22174.384	0.0000	.0024248	.001634	GLFC CONT.
310.2122	22128.908	0.0000	.0004696	.000229	GLFC CONT.
332.5960	22070.534	0.0000	.0000574	.000028	GLFC CONT.
355.0913	21999.332	0.0000	.0000091	.000004	GLFC CONT.
377.7205	21915.391	0.0000	.0000027	.000001	GLFC CONT.
400.5063	21818.811	0.0000	.0000012	.000001	GLFC CONT.
423.4724	21709.712	0.0000	.0000005	.000000	GLFC CONT.
446.6428	21588.225	0.0000	.0000003	.000000	GLFC CONT.

REVOLUTION 3

TIME	H R	QDOTR	QDOTC/H R	P T A	I. D.
0.0000	19888.518	0.0000	.0000004	.000000	GLFC CONT.
24.0201	19994.255	0.0000	.0000008	.000000	GLFC CONT.
47.8562	20089.210	0.0000	.0000017	.000001	GLFC CONT.
71.5299	20173.268	0.0000	.0000043	.000002	GLFC CONT.
95.0622	20246.327	0.0000	.0000166	.000008	GLFC CONT.
118.4737	20308.297	0.0000	.0001100	.000051	GLFC CONT.
141.7844	20359.103	0.0000	.0007866	.000368	GLFC CONT.
165.0136	20398.684	0.0000	.0027582	.002141	GLFC CONT.
188.1782	20426.990	0.0000	.0052623	.007791	GLFC CONT.
211.2823	20443.987	0.0000	.0076687	.016544	GLFC CONT.
232.7517	20449.655	0.0000	.0086743	.021167	GLFC CONT.
254.2211	20443.987	0.0000	.0076687	.016544	GLFC CONT.
277.3252	20426.990	0.0000	.0052623	.007791	GLFC CONT.
300.4898	20398.684	0.0000	.0027582	.002141	GLFC CONT.
323.7190	20359.103	0.0000	.0007866	.000368	GLFC CONT.
347.0298	20308.297	0.0000	.0001100	.000051	GLFC CONT.
370.4412	20246.327	0.0000	.0000166	.000008	GLFC CONT.
393.9735	20173.268	0.0000	.0000043	.000002	GLFC CONT.
417.6472	20089.210	0.0000	.0000017	.000001	GLFC CONT.
441.4833	19994.255	0.0000	.0000008	.000000	GLFC CONT.
465.5034	19888.518	0.0000	.0000004	.000000	GLFC CONT.

REVOLUTION 4

TIME	H R	QDOTR	QDOTC/H R	P T A	I. D.
0.0000	17942.224	0.0000	.0000008	.000000	GLFC CONT.
25.1280	18025.926	0.0000	.0000016	.000001	GLFC CONT.
50.1041	18101.093	0.0000	.0000036	.000002	GLFC CONT.
74.9458	18167.634	0.0000	.0000111	.000005	GLFC CONT.
99.6702	18225.467	0.0000	.0000546	.000024	GLFC CONT.
124.2944	18274.523	0.0000	.0003129	.000139	GLFC CONT.
148.8349	18314.741	0.0000	.0016161	.000747	GLFC CONT.
173.3078	18346.073	0.0000	.0033213	.003154	GLFC CONT.
197.7274	18368.480	0.0000	.0055032	.008658	GLFC CONT.
222.0991	18381.935	0.0000	.0074013	.015659	GLFC CONT.
245.0427	18386.422	0.0000	.0081597	.019031	GLFC CONT.
267.9862	18381.935	0.0000	.0074013	.015659	GLFC CONT.
292.3579	18368.480	0.0000	.0055032	.008658	GLFC CONT.
316.7775	18346.073	0.0000	.0033213	.003154	GLFC CONT.
341.2504	18314.741	0.0000	.0016161	.000747	GLFC CONT.
365.7909	18274.523	0.0000	.0003129	.000139	GLFC CONT.
390.4151	18225.467	0.0000	.0000546	.000024	GLFC CONT.
415.1395	18167.634	0.0000	.0000111	.000005	GLFC CONT.
439.9812	18101.093	0.0000	.0000036	.000002	GLFC CONT.
464.9573	18025.926	0.0000	.0000016	.000001	GLFC CONT.
490.0853	17942.224	0.0000	.0000008	.000000	GLFC CONT.

REVOLUTION 5

TIME	H_R	QDOTR	$QDOTC/H_R$	P_{TA}	I. D.
0.0000	15645.822	0.0000	.0000046	.000002	GLFC CONT.
26.6799	15695.522	0.0000	.0000114	.000005	GLFC CONT.
53.2644	15740.154	0.0000	.0000386	.000016	GLFC CONT.
79.7642	15779.665	0.0000	.0001481	.000061	GLFC CONT.
106.1900	15814.005	0.0000	.0005611	.000232	GLFC CONT.
132.5521	15843.133	0.0000	.0016704	.000816	GLFC CONT.
158.8611	15867.014	0.0000	.0029023	.002461	GLFC CONT.
185.1269	15885.618	0.0000	.0044238	.005718	GLFC CONT.
211.3586	15898.923	0.0000	.0059553	.010361	GLFC CONT.
237.5585	15906.912	0.0000	.0070857	.014666	GLFC CONT.
262.4999	15909.577	0.0000	.0075083	.016468	GLFC CONT.
287.4413	15906.912	0.0000	.0070857	.014666	GLFC CONT.
313.6413	15898.923	0.0000	.0059553	.010361	GLFC CONT.
339.8729	15885.618	0.0000	.0044238	.005718	GLFC CONT.
366.1387	15867.014	0.0000	.0029023	.002461	GLFC CONT.
392.4477	15843.133	0.0000	.0016704	.000816	GLFC CONT.
418.8099	15814.005	0.0000	.0005611	.000232	GLFC CONT.
445.2356	15779.665	0.0000	.0001481	.000061	GLFC CONT.
471.7354	15740.154	0.0000	.0000386	.000016	GLFC CONT.
498.3199	15695.522	0.0000	.0000114	.000005	GLFC CONT.
524.9998	15645.822	0.0000	.0000046	.000002	GLFC CONT.

APPENDIX D

Trajectory and Reentry Environment
Output From Computer Code HRS017 (Version 3)
for a Perigee Altitude of 265,000 Feet
(Ten Revolutions)

Part 1. Trajectory and Reentry Environment Tabulated Data (69)

Part 2. Listing of Punched Card CMA Input (79)

Part 1

Trajectory and Reentry Environment Tabulated Data

REVOLUTION 1

TIME	THETA	ALTITUDE	GAMMA	GCONT	QFM	VELOCITY	P/T
0.0	-180.00	1246374303.00	.08103	0.00	0.000	604.90	0.00000
385022.0	-160.00	436059651.60	74.58284	0.00	0.000	6310.07	0.00000
422283.7	-140.00	139923150.92	67.36965	0.00	0.000	12385.96	0.00000
428400.7	-120.00	59788203.95	58.34111	0.00	0.000	18095.57	0.00000
430261.0	-100.00	29171900.93	48.85844	0.00	0.000	23258.08	0.00000
431075.3	-80.00	14764927.90	39.19622	0.00	0.000	27715.13	0.00000
431529.6	-60.00	7171957.28	29.44699	0.00	0.000	31330.77	0.00000
431833.6	-40.00	3019182.55	19.65146	0.00	0.000	33994.92	0.00000
432069.4	-20.00	912491.03	9.83140	.39	.003	35626.53	.00014
432091.0	-18.00	787474.18	8.84863	.59	.007	35730.71	.00031
432112.4	-16.00	676418.28	7.86577	.90	.016	35824.01	.00070
432133.5	-14.00	579050.86	6.88284	1.37	.038	35906.40	.00163
432154.4	-12.00	495134.73	5.89986	2.27	.102	35977.85	.00442
432175.2	-10.00	424466.67	4.91685	4.88	.472	36038.35	.02036
432195.9	-8.00	366876.47	3.93384	14.82	4.324	36087.87	.18629
432216.4	-6.00	322226.02	2.95090	45.09	39.913	36126.41	1.71773
432236.8	-4.00	290408.60	1.96821	111.91	245.202	36153.94	10.54457
432256.7	-2.00	271348.38	.98661	191.40	716.133	36170.46	30.78227
432271.8	0.00	265000.00	.08103	227.89	1014.760	36175.97	43.61182
432286.8	2.00	271348.38	.98661	191.40	716.133	36170.46	30.78227
432306.8	4.00	290408.60	1.96821	111.91	245.202	36153.94	10.54457
432327.2	6.00	322226.02	2.95090	45.09	39.913	36126.41	1.71773
432347.7	8.00	366876.47	3.93384	14.82	4.324	36087.87	.18629
432368.3	10.00	424466.67	4.91685	4.88	.472	36038.35	.02036
432389.1	12.00	495134.73	5.89986	2.27	.102	35977.85	.00442
432410.1	14.00	579050.86	6.88284	1.37	.038	35906.40	.00163
432431.2	16.00	676418.28	7.86577	.90	.016	35824.01	.00070
432452.5	18.00	787474.18	8.84863	.59	.007	35730.71	.00031
432474.1	20.00	912491.03	9.83140	.39	.003	35626.53	.00014
432710.0	40.00	3019182.55	19.65146	0.00	0.000	33994.92	0.00000
433013.9	60.00	7171957.28	29.44699	0.00	0.000	31330.77	0.00000
433468.3	80.00	14764927.90	39.19622	0.00	0.000	27715.13	0.00000
434282.6	100.00	29171900.93	48.85844	0.00	0.000	23258.08	0.00000
436142.9	120.00	59788203.95	58.34111	0.00	0.000	18095.57	0.00000
442259.8	140.00	139923150.92	67.36965	0.00	0.000	12385.96	0.00000
479521.6	160.00	436059651.60	74.58284	0.00	0.000	6310.07	0.00000
864543.5	180.00	1246374303.00	.08103	0.00	0.000	604.90	0.00000

REVOLUTION 2

TIME	THETA	ALTITUDE	GAMMA	GCONT	QFM	VELOCITY	P_I
864543.5	-180.00	363668327.44	.08103	0.00	0.000	1956.67	0.00000
916776.0	-160.00	232578432.66	62.64699	0.00	0.000	6460.64	0.00000
932917.7	-140.00	107013257.18	61.39179	0.00	0.000	12284.19	0.00000
937356.9	-120.00	51813539.24	54.54858	0.00	0.000	17836.65	0.00000
938976.5	-100.00	26639412.72	46.24316	0.00	0.000	22875.80	0.00000
939743.6	-80.00	13836536.91	37.35298	0.00	0.000	27232.79	0.00000
940188.9	-60.00	6818998.39	28.17807	0.00	0.000	30769.81	0.00000
940493.2	-40.00	2898327.38	18.85129	0.00	0.000	33377.03	0.00000
940732.1	-20.00	886478.05	9.44371	.40	.003	34974.10	.00015
940754.1	-18.00	766599.12	8.50039	.60	.008	35076.08	.00034
940775.8	-16.00	660061.10	7.55676	.90	.017	35167.41	.00077
940797.3	-14.00	566618.88	6.61288	1.37	.040	35248.06	.00178
940818.6	-12.00	486058.78	5.66877	2.30	.112	35318.01	.00493
940839.8	-10.00	418197.63	4.72450	5.07	.540	35377.23	.02372
940860.9	-8.00	362881.83	3.78011	15.37	4.945	35425.71	.21702
940881.8	-6.00	319986.67	2.83571	45.17	42.563	35463.43	1.86599
940902.7	-4.00	289415.75	1.89149	108.59	245.431	35490.39	10.75176
940923.4	-2.00	271100.53	.94836	181.81	686.912	35506.56	30.07831
940940.9	0.00	265000.00	.08103	214.97	959.901	35511.95	42.02550
940958.5	2.00	271100.53	.94836	181.81	686.912	35506.56	30.07831
940979.2	4.00	289415.75	1.89149	108.59	245.431	35490.39	10.75176
941000.0	6.00	319986.67	2.83571	45.17	42.563	35463.43	1.86599
941021.0	8.00	362881.83	3.78011	15.37	4.945	35425.71	.21702
941042.0	10.00	418197.63	4.72450	5.07	.540	35377.23	.02372
941063.2	12.00	486058.78	5.66877	2.30	.112	35318.01	.00493
941084.6	14.00	566618.88	6.61288	1.37	.040	35248.06	.00178
941106.1	16.00	660061.10	7.55676	.90	.017	35167.41	.00077
941127.8	18.00	766599.12	8.50039	.60	.008	35076.08	.00034
941149.7	20.00	886478.05	9.44371	.40	.003	34974.10	.00015
941388.6	40.00	2898327.38	18.85129	0.00	0.000	33377.03	0.00000
941693.0	60.00	6818998.39	28.17807	0.00	0.000	30769.81	0.00000
942138.3	80.00	13836536.91	37.35298	0.00	0.000	27232.79	0.00000
942905.3	100.00	26639412.72	46.24316	0.00	0.000	22875.80	0.00000
944525.0	120.00	51813539.24	54.54858	0.00	0.000	17836.65	0.00000
948964.2	140.00	107013257.18	61.39179	0.00	0.000	12284.19	0.00000
965105.9	160.00	232578432.66	62.64699	0.00	0.000	6460.64	0.00000
1017338.3	180.00	363668327.44	.08103	0.00	0.000	1956.67	0.00000

REVOLUTION 3

TIME	THETA	ALTITUDE	GAMMA	CCONT	QEM	VELOCITY	P/T
1017338.3	-180.00	207448128.32	.08103	0.00	0.000	3237.81	0.00000
1038079.2	-160.00	155449935.76	52.24511	0.00	0.000	6847.08	0.00000
1047420.8	-140.00	85606797.36	55.69787	0.00	0.000	12316.23	0.00000
1050834.6	-120.00	45379740.53	50.86977	0.00	0.000	17670.97	0.00000
1052264.7	-100.00	24389682.80	43.68980	0.00	0.000	22566.26	0.00000
1052989.8	-80.00	12970605.84	35.54803	0.00	0.000	26811.38	0.00000
1053426.4	-60.00	6480884.39	26.93359	0.00	0.000	30262.57	0.00000
1053731.0	-40.00	2780817.46	18.06588	0.00	0.000	32808.49	0.00000
1053972.8	-20.00	860991.04	9.06301	.41	.004	34368.65	.00017
1053995.0	-18.00	746136.82	8.15842	.61	.008	34468.29	.00038
1054017.1	-16.00	644020.87	7.25331	.91	.019	34557.52	.00085
1054039.0	-14.00	554423.44	6.34777	1.38	.043	34636.32	.00194
1054060.7	-12.00	477152.81	5.44184	2.36	.125	34704.67	.00558
1054082.2	-10.00	412044.41	4.53560	5.30	.627	34762.53	.02804
1054103.6	-8.00	358960.16	3.62915	15.95	5.644	34809.90	.25206
1054125.0	-6.00	317787.87	2.72258	45.43	45.619	34846.76	2.03539
1054146.2	-4.00	288440.76	1.81615	105.60	245.934	34873.10	10.96451
1054167.3	-2.00	270857.12	.91081	173.21	660.652	34888.90	29.44058
1054185.9	0.00	265000.00	.08103	203.41	910.671	34894.17	40.57603
1054204.5	2.00	270857.12	.91081	173.21	660.652	34888.90	29.44058
1054225.6	4.00	288440.76	1.81615	105.60	245.934	34873.10	10.96451
1054246.9	6.00	317787.87	2.72258	45.43	45.619	34846.76	2.03539
1054268.2	8.00	358960.16	3.62915	15.95	5.644	34809.90	.25206
1054289.6	10.00	412044.41	4.53560	5.30	.627	34762.53	.02804
1054311.2	12.00	477152.81	5.44184	2.36	.125	34704.67	.00558
1054332.9	14.00	554423.44	6.34777	1.38	.043	34636.32	.00194
1054354.7	16.00	644020.87	7.25331	.91	.019	34557.52	.00085
1054376.8	18.00	746136.82	8.15842	.61	.008	34468.29	.00038
1054399.1	20.00	860991.04	9.06301	.41	.004	34368.65	.00017
1054640.8	40.00	2780817.46	18.06588	0.00	0.000	32808.49	0.00000
1054945.4	60.00	6480884.39	26.93359	0.00	0.000	30262.57	0.00000
1055382.0	80.00	12970605.84	35.54803	0.00	0.000	26811.38	0.00000
1056107.2	100.00	24389682.80	43.68980	0.00	0.000	22566.26	0.00000
1057537.3	120.00	45379740.53	50.86977	0.00	0.000	17670.97	0.00000
1060951.0	140.00	85606797.36	55.69787	0.00	0.000	12316.23	0.00000
1070292.7	160.00	155449935.76	52.24511	0.00	0.000	6847.08	0.00000
1091033.5	180.00	207448128.32	.08103	0.00	0.000	3237.81	0.00000

REVOLUTION 4

TIME	THETA	ALTITUDE	GAMMA	GCONT	QFM	VELOCITY	P/T
1091033.5	-180.00	131889268.85	.08103	0.00	0.000	4740.26	0.00000
1101061.0	-160.00	107782572.40	41.81746	0.00	0.000	7551.71	0.00000
1106765.0	-140.00	67580705.07	49.14371	0.00	0.000	12511.40	0.00000
1109367.9	-120.00	38934733.19	46.49448	0.00	0.000	17578.06	0.00000
1110612.8	-100.00	21922725.85	40.61622	0.00	0.000	22271.05	0.00000
1111292.2	-80.00	11973044.12	33.36316	0.00	0.000	26363.11	0.00000
1111718.5	-60.00	6080268.87	25.42275	0.00	0.000	29698.90	0.00000
1112023.2	-40.00	2639331.87	17.11084	0.00	0.000	32163.30	0.00000
1112268.2	-20.00	830046.87	8.59971	.42	.004	33674.69	.00021
1112290.9	-18.00	721280.84	7.74224	.63	.010	33771.24	.00044
1112313.4	-16.00	624527.81	6.88400	.93	.021	33857.71	.00096
1112335.7	-14.00	539597.05	6.02510	1.41	.048	33934.08	.00219
1112357.8	-12.00	466321.88	5.16562	2.45	.144	34000.31	.00660
1112379.8	-10.00	404559.10	4.30568	5.70	.774	34056.39	.03532
1112401.6	-8.00	354188.41	3.44539	16.69	6.611	34102.29	.30138
1112423.4	-6.00	315111.97	2.58489	45.86	49.756	34138.01	2.26605
1112445.1	-4.00	287254.07	1.72446	102.33	247.140	34163.54	11.24713
1112466.7	-2.00	270560.83	.86512	163.70	631.551	34178.85	28.72841
1112486.1	0.00	265000.00	.08103	190.65	856.190	34183.96	38.94113
1112505.5	2.00	270560.83	.86512	163.70	631.551	34178.85	28.72841
1112527.1	4.00	287254.07	1.72446	102.33	247.140	34163.54	11.24713
1112548.8	6.00	315111.97	2.58489	45.86	49.756	34138.01	2.26605
1112570.6	8.00	354188.41	3.44539	16.69	6.611	34102.29	.30138
1112592.5	10.00	404559.10	4.30568	5.70	.774	34056.39	.03532
1112614.4	12.00	466321.88	5.16562	2.45	.144	34000.31	.00660
1112636.6	14.00	539597.05	6.02510	1.41	.048	33934.08	.00219
1112658.9	16.00	624527.81	6.88400	.93	.021	33857.71	.00096
1112681.3	18.00	721280.84	7.74224	.63	.010	33771.24	.00044
1112704.0	20.00	830046.87	8.59971	.42	.004	33674.69	.00021
1112949.1	40.00	2639331.87	17.11084	0.00	0.000	32163.30	0.00000
1113253.7	60.00	6080268.87	25.42275	0.00	0.000	29698.90	0.00000
1113680.1	80.00	11973044.12	33.36316	0.00	0.000	26363.11	0.00000
1114359.4	100.00	21922725.85	40.61622	0.00	0.000	22271.05	0.00000
1115604.3	120.00	38934733.19	46.49448	0.00	0.000	17578.06	0.00000
1118207.2	140.00	67580705.07	49.14371	0.00	0.000	12511.40	0.00000
1123911.2	160.00	107782572.40	41.81746	0.00	0.000	7551.71	0.00000
1133938.7	180.00	131889268.85	.08103	0.00	0.000	4740.26	0.00000

REVOLUTION 5

TIME	THETA	ALTITUDE	GAMMA	CCONT	QFM	VELOCITY	P/T
1133938.7	-180.00	87661533.86	.08103	0.00	0.000	6511.43	0.00000
1139313.5	-160.00	75651011.76	32.09949	0.00	0.000	8642.40	0.00000
1142905.9	-140.00	52322794.85	41.80129	0.00	0.000	12948.85	0.00000
1144869.5	-120.00	32537317.29	41.32440	0.00	0.000	17610.49	0.00000
1145936.0	-100.00	19231464.77	36.90756	0.00	0.000	22019.94	0.00000
1146565.4	-80.00	10822806.47	30.70047	0.00	0.000	25900.61	0.00000
1146979.6	-60.00	5602889.25	23.57176	0.00	0.000	29079.03	0.00000
1147284.1	-40.00	2467457.87	15.93739	0.00	0.000	31433.21	0.00000
1147533.1	-20.00	792073.45	8.02963	.45	.005	32878.99	.00025
1147556.3	-18.00	690759.98	7.23008	.65	.011	32971.40	.00053
1147579.2	-16.00	600579.14	6.42948	.96	.024	33054.16	.00113
1147602.0	-14.00	521373.04	5.62796	1.45	.055	33127.25	.00259
1147624.7	-12.00	453003.48	4.82565	2.62	.178	33190.65	.00833
1147647.2	-10.00	395351.50	4.02268	6.32	1.031	33244.33	.04820
1147669.5	-8.00	348317.06	3.21920	17.75	8.099	33288.28	.37828
1147691.8	-6.00	311818.71	2.41540	46.56	55.550	33322.47	2.59186
1147714.1	-4.00	285793.37	1.61159	98.79	249.462	33346.91	11.63079
1147736.2	-2.00	270196.10	.80890	153.25	599.472	33361.57	27.93724
1147756.4	0.00	265000.00	.08103	176.66	796.220	33366.46	37.10086
1147776.7	2.00	270196.10	.80890	153.25	599.472	33361.57	27.93724
1147798.8	4.00	285793.37	1.61159	98.79	249.462	33346.91	11.63079
1147821.0	6.00	311818.71	2.41540	46.56	55.550	33322.47	2.59186
1147843.3	8.00	348317.06	3.21920	17.75	8.099	33288.28	.37828
1147865.7	10.00	395351.50	4.02268	6.32	1.031	33244.33	.04820
1147888.2	12.00	453003.48	4.82565	2.62	.178	33190.65	.00833
1147910.9	14.00	521373.04	5.62796	1.45	.055	33127.25	.00259
1147933.6	16.00	600579.14	6.42948	.96	.024	33054.16	.00113
1147956.6	18.00	690759.98	7.23008	.65	.011	32971.40	.00053
1147979.8	20.00	792073.45	8.02963	.45	.005	32878.99	.00025
1148228.7	40.00	2467457.87	15.93739	0.00	0.000	31433.21	0.00000
1148533.2	60.00	5602889.25	23.57176	0.00	0.000	29079.03	0.00000
1148947.5	80.00	10822806.47	30.70047	0.00	0.000	25900.61	0.00000
1149576.9	100.00	19231464.77	36.90756	0.00	0.000	22019.94	0.00000
1150643.4	120.00	32537317.29	41.32440	0.00	0.000	17610.49	0.00000
1152607.0	140.00	52322794.85	41.80129	0.00	0.000	12948.85	0.00000
1156199.4	160.00	75651011.76	32.09949	0.00	0.000	8642.40	0.00000
1161574.2	180.00	87661533.86	.08103	0.00	0.000	6511.43	0.00000

REVOLUTION 6

TIME	THETA	ALTITUDE	GAMMA	QCONT	QFM	VELOCITY	P_T
1161574.2	-180.00	58896432.89	.08103	0.00	0.000	8608.28	0.00000
1164636.0	-160.00	52749648.68	23.59212	0.00	0.000	10177.09	0.00000
1166939.6	-140.00	39378419.23	33.89348	0.00	0.000	13727.00	0.00000
1168402.6	-120.00	26258535.02	35.30643	0.00	0.000	17844.88	0.00000
1169299.9	-100.00	16318760.30	32.44378	0.00	0.000	21861.37	0.00000
1169875.6	-80.00	9498345.99	27.44199	0.00	0.000	25448.66	0.00000
1170275.4	-60.00	5031572.52	21.28615	0.00	0.000	28409.75	0.00000
1170579.4	-40.00	2256925.65	14.48117	.01	.000	30612.46	.00000
1170832.9	-20.00	744976.59	7.32037	.48	.007	31968.43	.00033
1170856.7	-18.00	652877.71	6.59280	.69	.014	32055.16	.00068
1170880.2	-16.00	570834.30	5.86385	1.01	.029	32132.86	.00142
1170903.6	-14.00	498725.04	5.13368	1.55	.069	32201.48	.00335
1170926.9	-12.00	436443.53	4.40247	2.92	.243	32261.00	.01172
1170950.0	-10.00	383897.96	3.67038	7.25	1.492	32311.41	.07178
1170973.0	-8.00	341011.01	2.93761	19.41	10.646	32352.67	.51160
1170995.9	-6.00	307719.62	2.20439	47.83	64.411	32384.78	3.09231
1171018.8	-4.00	283974.90	1.47108	95.01	253.560	32407.72	12.16446
1171041.6	-2.00	269741.99	.73896	141.82	564.176	32421.49	27.05470
1171062.7	0.00	265000.00	.08103	161.44	730.780	32426.09	35.03909
1171083.8	2.00	269741.99	.73896	141.82	564.176	32421.49	27.05470
1171106.6	4.00	283974.90	1.47108	95.01	253.560	32407.72	12.16446
1171129.5	6.00	307719.62	2.20439	47.83	64.411	32384.78	3.09231
1171152.4	8.00	341011.01	2.93761	19.41	10.646	32352.67	.51160
1171175.4	10.00	383897.96	3.67038	7.25	1.492	32311.41	.07178
1171198.5	12.00	436443.53	4.40247	2.92	.243	32261.00	.01172
1171221.8	14.00	498725.04	5.13368	1.55	.069	32201.48	.00335
1171245.2	16.00	570834.30	5.86385	1.01	.029	32132.86	.00142
1171268.7	18.00	652877.71	6.59280	.69	.014	32055.16	.00068
1171292.5	20.00	744976.59	7.32037	.48	.007	31968.43	.00033
1171546.0	40.00	2256925.65	14.48117	.01	.000	30612.46	.00000
1171850.0	60.00	5031572.52	21.28615	0.00	0.000	28409.75	0.00000
1172249.8	80.00	9498345.99	27.44199	0.00	0.000	25448.66	0.00000
1172825.5	100.00	16318760.30	32.44378	0.00	0.000	21861.37	0.00000
1173722.8	120.00	26258535.02	35.30643	0.00	0.000	17844.88	0.00000
1175185.8	140.00	39378419.23	33.89348	0.00	0.000	13727.00	0.00000
1177489.4	160.00	52749648.68	23.59212	0.00	0.000	10177.09	0.00000
1180551.2	180.00	58896432.89	.08103	0.00	0.000	8608.28	0.00000

REVOLUTION 7

TIME	THETA	ALTITUDE	GAMMA	GCONT	QFM	VELOCITY	P/T
1180551.2	-180.00	38802358.92	.08103	0.00	0.000	11118.66	0.00000
1182356.3	-160.00	35697298.43	16.42734	0.00	0.000	12227.51	0.00000
1183843.0	-140.00	28324986.88	25.73218	0.00	0.000	14968.35	0.00000
1184915.5	-120.00	20134404.06	28.42905	0.00	0.000	18391.64	0.00000
1185654.5	-100.00	13177320.83	27.08060	0.00	0.000	21871.00	0.00000
1186172.4	-80.00	7967559.19	23.42181	0.00	0.000	25048.34	0.00000
1186555.0	-60.00	4340528.54	18.42406	0.00	0.000	27703.93	0.00000
1186858.0	-40.00	1994951.09	12.64227	.02	.000	29693.58	.00000
1187116.8	-20.00	685457.39	6.42084	.54	.010	30923.27	.00049
1187141.3	-18.00	604958.33	5.78435	.77	.019	31002.04	.00096
1187165.6	-16.00	533176.73	5.14612	1.11	.040	31072.61	.00198
1187189.7	-14.00	470031.02	4.50637	1.79	.103	31134.95	.00513
1187213.7	-12.00	415449.39	3.86530	3.56	.405	31189.03	.02018
1187237.6	-10.00	369369.74	3.22314	8.86	2.491	31234.82	.12397
1187261.4	-8.00	331739.58	2.58011	22.21	15.590	31272.32	.77507
1187285.1	-6.00	302516.07	1.93649	49.99	78.737	31301.50	3.91087
1187308.7	-4.00	281665.89	1.29272	91.05	260.582	31322.36	12.93455
1187332.3	-2.00	269165.29	.65025	129.40	525.585	31334.87	26.07811
1187354.4	0.00	265000.00	.08103	145.00	659.721	31339.04	32.72919
1187376.4	2.00	269165.29	.65025	129.40	525.585	31334.87	26.07811
1187400.0	4.00	281665.89	1.29272	91.05	260.582	31322.36	12.93455
1187423.7	6.00	302516.07	1.93649	49.99	78.737	31301.50	3.91087
1187447.4	8.00	331739.58	2.58011	22.21	15.590	31272.32	.77507
1187471.2	10.00	369369.74	3.22314	8.86	2.491	31234.82	.12397
1187495.1	12.00	415449.39	3.86530	3.56	.405	31189.03	.02018
1187519.1	14.00	470031.02	4.50637	1.79	.103	31134.95	.00513
1187543.2	16.00	533176.73	5.14612	1.11	.040	31072.61	.00198
1187567.5	18.00	604958.33	5.78435	.77	.019	31002.04	.00096
1187591.9	20.00	685457.39	6.42084	.54	.010	30923.27	.00049
1187850.8	40.00	1994951.09	12.64227	.02	.000	29693.58	.00000
1188153.7	60.00	4340528.54	18.42406	0.00	0.000	27703.93	0.00000
1188536.4	80.00	7967559.19	23.42181	0.00	0.000	25048.34	0.00000
1189054.3	100.00	13177320.83	27.08060	0.00	0.000	21871.00	0.00000
1189793.2	120.00	20134404.06	28.42905	0.00	0.000	18391.64	0.00000
1190865.7	140.00	28324986.88	25.73218	0.00	0.000	14968.35	0.00000
1192352.5	160.00	35697298.43	16.42734	0.00	0.000	12227.51	0.00000
1194157.5	180.00	38802358.92	.08103	0.00	0.000	11118.66	0.00000

REVOLUTION 8

TIME	THETA	ALTITUDE	GAMMA	GCONT	QFM	VELOCITY	P_T
1194157.5	-180.00	23945739.44	.08103	0.00	0.000	14197.28	0.00000
1195233.5	-160.00	22482998.98	10.47461	0.00	0.000	14924.37	0.00000
1196186.0	-140.00	18758133.30	17.62196	0.00	0.000	16843.57	0.00000
1196953.3	-120.00	14147194.10	20.71811	0.00	0.000	19419.46	0.00000
1197544.9	-100.00	9771857.79	20.62891	0.00	0.000	22174.29	0.00000
1198000.8	-80.00	6174186.52	18.38334	0.00	0.000	24771.70	0.00000
1198362.5	-60.00	3485765.35	14.74891	0.00	0.000	26985.57	0.00000
1198663.4	-40.00	1659274.20	10.24727	.03	.000	28664.10	.00000
1198928.6	-20.00	607671.28	5.24053	.66	.016	29708.57	.00086
1198954.0	-18.00	542255.90	4.72307	.92	.031	29775.65	.00164
1198979.1	-16.00	483848.38	4.20358	1.38	.070	29835.76	.00366
1199004.2	-14.00	432408.28	3.68228	2.42	.215	29888.86	.01118
1199029.1	-12.00	387899.79	3.15945	5.27	1.014	29934.95	.05267
1199054.0	-10.00	350291.75	2.63531	12.16	5.371	29973.98	.27860
1199078.7	-8.00	319557.73	2.11015	27.00	26.402	30005.94	1.36803
1199103.4	-6.00	295676.03	1.58431	53.53	103.484	30030.82	5.35755
1199128.1	-4.00	278629.76	1.05830	86.99	272.802	30048.60	14.11513
1199152.7	-2.00	268406.83	.53389	115.89	483.547	30059.27	25.01041
1199175.9	0.00	265000.00	.08103	127.20	582.361	30062.83	30.11781
1199199.1	2.00	268406.83	.53389	115.89	483.547	30059.27	25.01041
1199223.7	4.00	278629.76	1.05830	86.99	272.802	30048.60	14.11513
1199248.3	6.00	295676.03	1.58431	53.53	103.484	30030.82	5.35755
1199273.0	8.00	319557.73	2.11015	27.00	26.402	30005.94	1.36803
1199297.8	10.00	350291.75	2.63531	12.16	5.371	29973.98	.27860
1199322.6	12.00	387899.79	3.15945	5.27	1.014	29934.95	.05267
1199347.6	14.00	432408.28	3.68228	2.42	.215	29888.86	.01118
1199372.6	16.00	483848.38	4.20358	1.38	.070	29835.76	.00366
1199397.8	18.00	542255.90	4.72307	.92	.031	29775.65	.00164
1199423.2	20.00	607671.28	5.24053	.66	.016	29708.57	.00086
1199688.4	40.00	1659274.20	10.24727	.03	.000	28664.10	.00000
1199989.3	60.00	3485765.35	14.74891	0.00	0.000	26985.57	0.00000
1200351.0	80.00	6174186.52	18.38334	0.00	0.000	24771.70	0.00000
1200806.8	100.00	9771857.79	20.62891	0.00	0.000	22174.29	0.00000
1201398.5	120.00	14147194.10	20.71811	0.00	0.000	19419.46	0.00000
1202165.7	140.00	18758133.30	17.62196	0.00	0.000	16843.57	0.00000
1203118.2	160.00	22482998.98	10.47461	0.00	0.000	14924.37	0.00000
1204194.3	180.00	23945739.44	.08103	0.00	0.000	14197.28	0.00000